

# UTAH COMMINATION CENTER

University of Utah  
306 W.C. Browning Building  
Salt Lake City, UT 84112

## COMPUTER SIMULATION OF TACONITE GRINDING AND CONCENTRATION CIRCUITS

Report Number II:           Characterization of Taconite Ore and  
Simulation of the Fairlane Plant  
Secondary Grinding Circuit

R. P. King and C. L. Schneider  
Comminution Center  
306 W.C. Browning Building  
University of Utah  
Salt Lake City, UT 84112

August 1995

## TABLE OF CONTENTS

Computer Simulation of Taconite Grinding and Concentration Circuits . . . . .	1
Introduction . . . . .	1
Fairlane Grinding Circuit . . . . .	3
Experimental . . . . .	5
Sampling . . . . .	6
Solids Content . . . . .	7
Size Analysis and Separation . . . . .	9
Specimen Preparation . . . . .	9
Image Acquisition . . . . .	12
Image Processing and Measurements . . . . .	13
The Conditional, on size, Volumetric Grade Distributions . . . . .	18
Texture and Phase Characterization . . . . .	21
MODSIM Simulation Setup and Models . . . . .	42
Liberation Model . . . . .	45
Comminution Model . . . . .	49
Wet Magnetic Drum Separator Model . . . . .	50
Hydrocyclone Classification Model . . . . .	53
MODSIM Simulation Results . . . . .	56
Discussion . . . . .	61
Summary and Conclusions . . . . .	73
Future Work . . . . .	76
Appendix: Measured Linear Grade Distributions in the Taconite Ore Samples	
From the Fairlane Plant Secondary Grinding Circuit . . . . .	77
References . . . . .	88

## **Summary and Conclusions**

Modern mineral processing plant simulation techniques can be used to minimize energy consumption while maximizing recovery of iron content from Taconite ore bodies. Essential to such study is the detailed and accurate characterization of the comminution and liberation properties of the Taconite and the accurate calibration of each of the unit operations in the grinding and concentration circuits. This report covers both the characterization of the comminution and liberation properties of the Taconite ore and the calibration of each of the unit operations in the Fairlane Plant secondary grinding circuit. The Taconite ore is very favorable for liberation studies, with respect to composition and texture. The sampling campaign at the Fairlane Plant was successful and the results in general are excellent.

The following conclusions can be drawn from this campaign.

1. The work reported here demonstrates that it is possible to model accurately the liberation of the minerals in the Fairlane Plant secondary grinding circuit.
2. A few empirical parameters are required to model the unit operations in the circuit. These parameters can be determined from the measured size/grade spectra in the circuit streams, with the selection of appropriate models and an optimization procedure.
3. The mineralogical texture of the Taconite ore was characterized completely by direct observation using image analysis. These results are not restricted, and can be used for any ore body in the Mesabi Iron Range of similar formation.
4. This study demonstrated that it is possible to measure the liberation spectra accurately in many size fractions in several plant streams using standard image analysis techniques with stereological correction. These spectra were used to confirm the validity

of the simulation and provided immediate indications of where improvements in the overall plant performance might be sought.

5. The simulator can form the basis for the determination of an overall economic optimum for the process as a whole.

### **Future Work**

Potential for reduction of mill power draft in the plant has been determined. The detailed characterization reported here has indicated two separate sources of potential improvement. The first issue to be addressed is the reconfiguration of the Dewatering Drum streams, which may represent a reduction of up to 10% of mill power draft. The second issue is with respect to the recirculation of liberated magnetite in the hydrocyclone underflow. It is possible, by setting appropriate operational conditions, that the amount of recirculating liberated and nearly liberated magnetite be reduced by a significant fraction, with proportional reduction of the power draft of the mill. The simulator will be used to assess these issues.

# COMPUTER SIMULATION OF TACONITE GRINDING AND CONCENTRATION CIRCUITS

## Introduction

The work reported here originated from a research program sponsored by Minnesota Power with the intention of minimizing the use of energy in the Taconite Industry in Minnesota, which produces iron pellets for steel making. Because the cost of comminution represents a significant fraction of the total cost of pellet production, the potential for improved economic performance is quite large if improvements in comminution efficiency should be possible by evolutionary improvement in existing Taconite comminution circuits. This work was dedicated to the preliminary characterization of the mineralogical texture of the Taconite ore and the characterization of a typical Taconite grinding and classification circuit, since these are the most crucial operations. The Taconite ore constitutes a typical ore with problematic liberation characteristics, which requires comminution to comparatively fine sizes so that enough Magnetite, the main iron bearing mineral, is liberated from the Chert (micro-crystalline quartz) matrix. Chert is known to be abrasive, tough material, and this contributes to the relatively high cost of Taconite processing. As a result of the combined liberation and comminution characteristics of the Minnesota Taconite, the American pellet producing industry has been suffering harsh competition from other countries which produce pellets from richer, easier to process ores such as the Itabirito in Brazil, an ore rich in Hematite

that has much more favorable comminution and liberation characteristics.

The grinding circuit of the Fairlane Plant, located at mile 4 on county road 17, south of Eveleth, was chosen to be the subject of this study. The plant processes a blend of Taconite ore that is mined by Eveleth Mines at the Thunderbird North Mine, from four mining horizons denominated Middle Upper Cherty, Lower Upper Cherty, Top Lower Cherty and Bottom Lower Cherty, which present a magnetite content above cutoff grade. The plant produces pellets containing not more than 5.30%  $\text{SiO}_2$  and 78 to 82% of the particles in the pellets should pass the 45 microns screen.

The study carried out in the Fairlane Plant provided with an excellent opportunity to test, in practice, the procedures and models previously described in this work. The Taconite ore is a typical case for which the symmetric transformation kernel for stereological correction can be used, since the exact transformation kernel for the Taconite ore is not known. The symmetric transformation kernel is tested here as an approximate transformation kernel that can be used for typical ores in the preliminary assessment of the liberation spectra of the ore at several particle sizes. The preliminary characterization of the mineralogical texture of the ore was carried out by fractionating a narrow size sample obtained from the plant into a few grade intervals. This procedure provided enough information to estimate the density of the two relevant phases in the ore, Magnetite and Chert, and, through the measurement of interphase area per unit volume of phase, a good estimate of the geometrical texture parameter  $\phi$ , at that size range, was obtained.

The bulk of the experimental work consisted of the measurement of the size

spectra, by standard sieving, and the liberation spectra, by image analysis, in every stream in the secondary grinding circuit of the Fairlane plant. These data were used to develop appropriate models for use with MODSIM, and to test the application of the liberation model developed in this work for an ore other than Dolomite-Sphalerite.

#### Fairlane Plant Grinding Circuit

The simplified flowsheet of the plant's secondary grinding circuit is shown in Figure 1. The grinding circuit feed is mainly the concentrate stream of Cobber Magnetic Separators, which concentrate Rod Mill discharge in the primary grinding stage. For this particular circuit, Ball Mill grinding is performed in closed circuit with both classification and concentration. The Ball Mill is 12.81 meters long by 5.185 meters in diameter (42 by 17 feet), and is equipped with rectangular lifters that are 76.2 millimeters high. Grinding media is fed to the Ball Mill at a rate of 2724 kilograms (6000 pounds) per day. The nominal mill charge represents 36% filling by volume, and the grinding media is constituted by 60% of 50.8 millimeters (2 inches) balls and 40% of 38.1 millimeters (1.5 inches) balls. The Ball Mill revolves at 12 *RPM*, which is 64% of critical speed.

Most of the concentration is carried out in wet magnetic drum separators which are fed directly with the ball mill discharge stream. This separation is designated as Rougher, and its concentrate/magnetic stream is the major component of the cyclone feed stream. The Rougher tails are subject to further concentration, and the concentrate of the Scavenger separation is returned to the grinding circuit through the cyclone feed stream.

The major classification stage is performed in four KREBS hydrocyclones

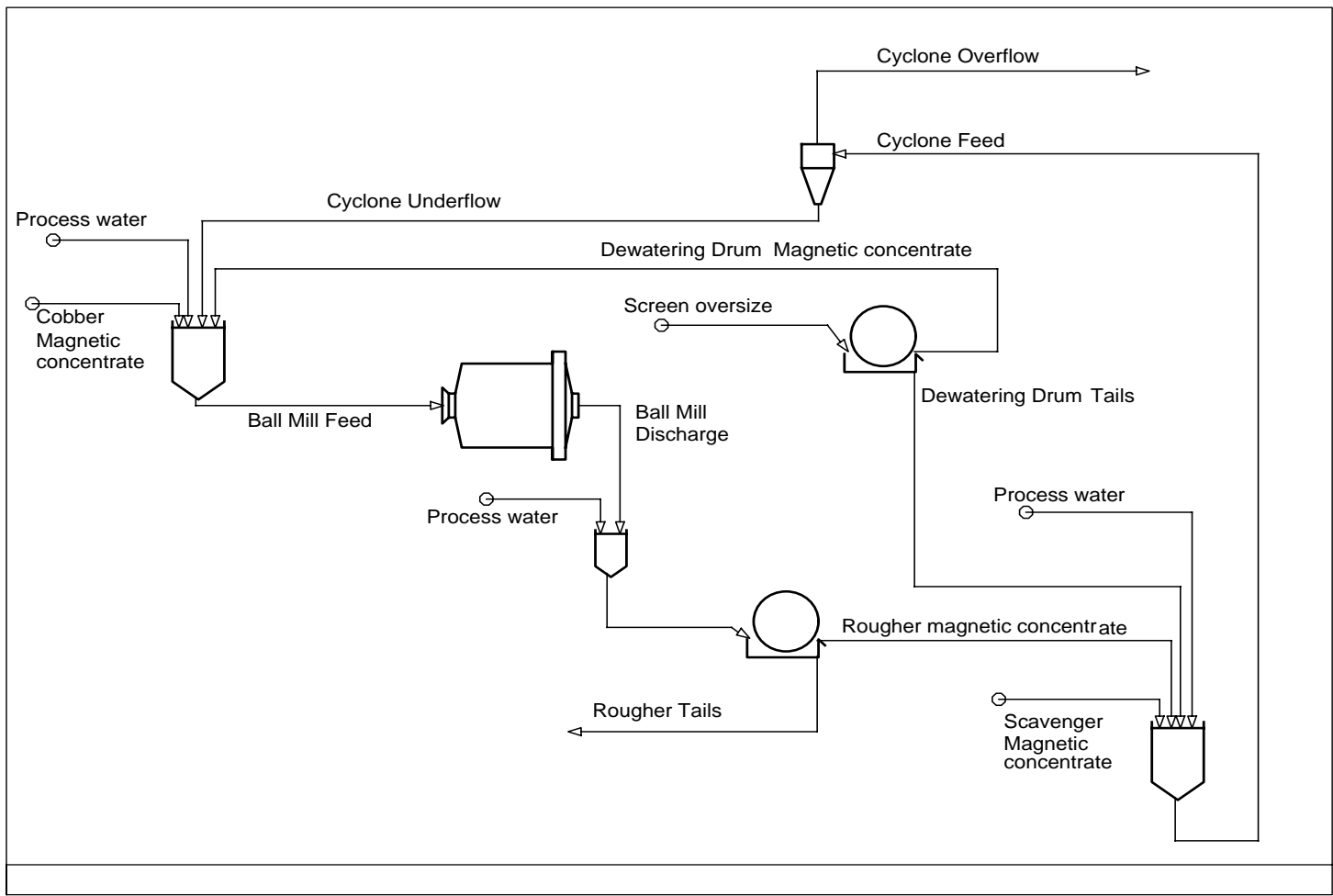


Figure 1 The simplified secondary grinding circuit flowsheet at the Fairlane Plant

assembled in a cluster. The hydrocyclones are 660 millimeters (26 inches) in diameter. The circular inlets measure 241.3 millimeters (9.5 inches). Vortex finder length is 279.4 millimeters (11 inches) and the spigot-vortex finder distance measures 2082.8 millimeters (82 inches). Spigot diameter is 114.3 millimeters (4.5 inches). The cyclone underflow is recirculated to the ball mills and the cyclone overflow constitutes the product of the secondary grinding circuit. The cyclone overflow is fed to a hydro separator, and the concentrate product of the hydro separator is screened in fine, double deck, vibrating screens, with primary opening of 150 microns (0.006 inches) and secondary opening of 100 microns (0.004 inches). The screens oversize is split in two fractions. One fraction is fed to a regrind circuit. The other fraction, representing approximately 5/6 of the screens oversize, is returned to the grinding circuit through a wet magnetic drum separator. The major role of this separation stage is dewatering, and a magnetic/concentrate stream is produced that contains mostly solids. This is then recirculated to the ball mills. The tail stream is mostly water, which is recirculated to the cyclones. This separation stage is designated as the Dewatering Drum.

## **Experimental**

The experimental work started with the sampling of the Fairlane Plant secondary grinding circuit streams. This was followed by solids contents measurement, which was the only measurement carried out at the plant site. The particle size distributions were carefully determined in each stream and a sample from each size range below 1000 microns was separated for image analysis. These were mounted, ground, polished and coated. A set of images from each specimen was acquired. The images were processed

for chord length distribution and linear grade distribution measurements. A larger narrow size sample from the Ball Mill Discharge was used for texture and phase characterization by fractionation.

### Sampling

Sampling of the Fairlane Plant grinding circuit was carried out on 11/16/1993. The selected streams were sampled in the order given below, according to the location of the sampling points in the plant, to minimize the time necessary for sampling. The corresponding abbreviated names, as used in the tables and figures, are listed along the stream names.

- Cobber Concentrate, Cob.Conc.
- Cyclone Feed, Cyc.Feed
- Cyclone Underflow, Cyc.Under
- Cyclone Overflow, Cyc.Over
- Dewatering Drum Concentrate, D.D.Conc.
- Dewatering Drum Tails, D.D.Tails
- Ball Mill Discharge, B.M.Disch.
- Rougher Concentrate, Rough.Conc.
- Rougher Tails, Rough.Tails
- Scavenger Concentrate, Scav.Conc.

The samples were collected with sample cutters in all streams. Three rounds were carried out following the sequence above, with no time interval between rounds. Each round consumed an average 20 minutes time. The samples from each round were added,

producing one composite sample for each stream. The pressure head in the cyclone cluster was measured for each round. There are four cyclones in the cluster and two cyclones were operating at sampling time while the other two were standing by. Pressure heads in each round were 843.6, 949.1 and 949.1 g cm<sup>-2</sup> (12.0, 13.5 and 13.5 PSIG), in that order. The samples were collected from open streams, and in most cases the sample cutter used was long enough so that the sample obtained was representative of the entire stream. The exception was the sample collected at the ball mill discharge, where the flow rate was too high so that the cutter could not be held steadily during sampling, neither could it be inserted deeply enough into the stream. However, an effort was made to obtain the best possible sample. The Cyclone Feed sample was drawn with a probe from the cluster feed head. The sampling at that particular point is routinely performed at the plant, and the probe depth to obtain a representative sample from well-mixed slurry had previously been established.

### Solids Content

Each sample was immediately weighed after sampling, and the wet weight noted. The samples were then filtered, dried and cooled to room temperature. The solids weight was then measured and noted. The solids content by weight, for each stream, is shown in Table 1. The samples were then bagged and labeled, completing the work at the plant site.

Table 1 Measured solids content in the sampled streams

Stream	Weight Wet, g	Weight Dry, g	Solids, %
Cobber Concentrate	6647.7	4224.0	63.54
Cyclone Feed	2229.5	1091.5	48.96
Cyclone Underflow	4536.4	3627.0	79.95
Cyclone Overflow	5763.6	1833.0	31.80
Dewatering Drum Conc.	3463.6	2104.5	60.76
Dewatering Drum Tails	13500.0	562.5	4.17
Ball Mill Discharge	7247.7	4954.6	68.36
Rougher Concentrate	4472.7	2951.0	65.98
Rougher Tails	9311.4	562.5	6.04
Scavenger Concentrate	2632.0	213.5	8.11

## Size Analysis and Separation

The samples were separated in narrow size intervals by screening. This was carried out in a disliming, wet screening stage, followed by dry screening. Each sample was first wet screened at 150 microns. The undersize fractions, (-150 microns), were wet screened with a 38 microns sieve, until no particles passed through. After filtering and drying, the dislimed fractions, (+38 microns), were dry screened with the aid of a ROTAP™, into several narrow size fractions. Each narrow size sample was weighted and bagged individually with the proper identification label, to follow specimen preparation for image analysis. The resulting size distributions and the size intervals used are shown in Table 2. The size distributions around the two major nodes in the circuit, namely the rougher concentration and the hydrocyclone classification, must be consistent so that the units can be parameterized properly. The raw measured size distributions are not exact, and the error is due to sampling inaccuracy that is inherent to sampling high flowrate streams in industrial plants. Material balance smoothing was carried out around the two nodes using MASSBAL, a material balance smoothing package developed by Kenwalt Systems [1]. The amount of smoothing required was minimal, indicating that the sampling procedure was good. The resulting smoothed size distributions in the corresponding streams are shown in Table 3.

## Specimen Preparation

The fractions below 1000 microns, whenever available in enough quantity, were mounted in epoxide resin for image analysis. A representative sample of about 6 grams from each size fraction was separated in a PULVERIT™ automatic sampler. Each

Table 2 Measured cumulative size distributions in the sampled streams

Size, microns		Fairlane Plant grinding circuit sampled streams									
Upper	Lower	B.M. Disch.	Cob. Conc.	Cyc. Feed	Cyc. Over	Cyc. Under	D.D. Conc.	D.D. Tails	Rough. Conc.	Rough. Tails	Scav. Conc.
9600	8000	1.0000	1.0000	1.0000	1.0000	1.0000	1.0000	1.0000	1.0000	1.0000	1.0000
8000	6300	1.0000	0.9991	1.0000	1.0000	1.0000	1.0000	1.0000	1.0000	1.0000	1.0000
6300	5600	0.9999	0.9955	0.9996	1.0000	0.9994	1.0000	1.0000	1.0000	1.0000	1.0000
5600	4750	0.9998	0.9922	0.9996	1.0000	0.9992	1.0000	1.0000	0.9997	1.0000	1.0000
4750	3350	0.9995	0.9836	0.9996	1.0000	0.9988	1.0000	1.0000	0.9995	1.0000	1.0000
3350	2800	0.9984	0.9357	0.9993	1.0000	0.9966	1.0000	1.0000	0.9981	0.9993	1.0000
2800	2000	0.9969	0.8872	0.9986	1.0000	0.9937	1.0000	1.0000	0.9968	0.9991	1.0000
2000	1400	0.9925	0.7742	0.9967	1.0000	0.9844	1.0000	1.0000	0.9921	0.9982	1.0000
1400	1000	0.9831	0.6538	0.9914	0.9999	0.9661	0.9998	1.0000	0.9832	0.9964	0.9995
1000	710	0.9691	0.5356	0.9828	0.9997	0.9403	0.9993	0.9997	0.9703	0.9939	0.9981
710	500	0.9466	0.4340	0.9662	0.9993	0.8988	0.9983	0.9993	0.9497	0.9898	0.9967
500	355	0.9150	0.3606	0.9445	0.9987	0.8429	0.9967	0.9986	0.9206	0.9841	0.9953
355	250	0.8699	0.2986	0.9037	0.9963	0.7663	0.9914	0.9956	0.8762	0.9681	0.9910
250	180	0.8103	0.2478	0.8398	0.9901	0.6671	0.9813	0.9834	0.8119	0.9367	0.9858
180	106	0.7304	0.2116	0.7620	0.9752	0.5419	0.9520	0.9114	0.7317	0.8932	0.9715
106	75	0.5560	0.1668	0.5883	0.8862	0.3308	0.7607	0.5209	0.5622	0.7826	0.7973
75	53	0.3151	0.1379	0.4442	0.7692	0.1414	0.5063	0.2849	0.3725	0.6892	0.5662
53	45	0.2524	0.1107	0.3290	0.5979	0.0925	0.3610	0.1908	0.2758	0.5991	0.4025
45	38	0.2432	0.1003	0.2915	0.5426	0.0780	0.3262	0.1705	0.2510	0.5615	0.3441
38	0	0.2208	0.0805	0.2496	0.4908	0.0573	0.2967	0.1463	0.2165	0.5285	0.2990

Table 3 Adjusted cumulative size distributions in the streams corresponding to the two main circuit nodes

Size, microns		Cumulative Size Distributions in Stream					
Upper	Lower	Cyc. Feed	Cyc. Over	Cyc. Under	B.M. Disch.	Rough. Conc.	Rough. Tails
9600	8000	1.0000	1.0000	1.0000	1.0000	1.0000	1.0000
8000	6300	1.0000	1.0000	0.9999	1.0000	1.0000	1.0000
6300	5600	0.9996	1.0000	0.9993	1.0000	1.0000	1.0000
5600	4750	0.9996	1.0000	0.9993	0.9998	0.9982	1.0000
4750	3350	0.9996	1.0000	0.9993	0.9996	0.9980	1.0000
3350	2800	0.9993	1.0000	0.9987	0.9983	0.9966	0.9993
2800	2000	0.9984	1.0000	0.9972	0.9971	0.9953	0.9991
2000	1400	0.9961	1.0000	0.9932	0.9926	0.9905	0.9982
1400	1000	0.9895	0.9999	0.9822	0.9840	0.9813	0.9964
1000	710	0.9790	0.9997	0.9645	0.9715	0.9679	0.9939
710	500	0.9593	0.9994	0.9312	0.9516	0.9464	0.9897
500	355	0.9333	0.9989	0.8875	0.9234	0.9161	0.9840
355	250	0.8884	0.9966	0.8128	0.8802	0.8705	0.9679
250	180	0.8233	0.9906	0.7064	0.8182	0.8057	0.9364
180	106	0.7412	0.9763	0.5769	0.7395	0.7238	0.8926
106	75	0.5697	0.8903	0.3457	0.5709	0.5500	0.7813
75	53	0.4121	0.7804	0.1547	0.3797	0.3500	0.6872
53	45	0.3082	0.6047	0.1009	0.2829	0.2602	0.5973
45	38	0.2752	0.5474	0.0849	0.2739	0.2461	0.5619
38	0	0.2394	0.4937	0.0617	0.2430	0.2155	0.5291

representative sample was again wet sieved before mounting, to avoid even the slightest contamination of smaller particles and slime. After drying at room temperature, the particles were placed under weak vacuum in a lab desiccator. After approximately 10 minutes under vacuum, the particles were carefully mounted in epoxide resin, with the proper label identifying the stream and the size range. The sample mounts, totaling 105, were ground in an automatic grinding head, with an 125 microns diamond grinding disc at 120 *RPM*, 2.3 kg/sample pressure, and counter-clockwise grinding head motion, until between 1 and 2 millimeters of material had been ground off the specimen surface. Diamond grinding is essential due to the hardness of the micro-crystalline silica (Chert). This was followed by grinding with 40 microns and 6 microns diamond grinding discs, at the same settings, until the specimen surface was fairly smooth. Polishing followed manually, by lapping with 9 micron and then 1 micron diamond slurry at 200 *RPM*. The final polish was carried out by lapping with 0.3 micron alumina, at 600 *RPM*. After polishing, each specimen surface was coated with a film of carbon for image acquisition in the *SEM*.

### Image Acquisition

Whenever possible, 30 backscattered electron images were collected from each specimen using the *SEM*. Magnification was kept proportional to particle size. Image collection followed a pattern on the specimen surface such that each point on the surface had an equal probability of being scanned. Care was taken to avoid image overlapping. Scanning speed was kept at 0.25 Frames/second and a 16 frame true average image was collected to eliminate noise. The 3004 images were generated at high resolution

(2048x2048 frames) and stored in tapes, after high resolution stretching and compressing, in 512x512 format, as raw binary files.

### Image Processing and Measurements

The processing of each image started with background correction to grey level 40, for the Taconite ore, followed by delineation filtering. A typical image is shown in Figure 2, after background correction and delineation filtering. This image was collected from -500+355 micron particles from the Cyclone Underflow stream. The magnification used for this particular image was 50X. The grey level histogram for this image is shown in Figure 3. The left peak in the histogram corresponds to the darkest phase in the image, which is the backscattered electron intensities detected from the epoxy mounting media. The following peaks at higher grey levels are backscattered electron intensities detected from the particles. Two major components are readily identified, one brighter, corresponding to the peak at the right of the histogram, and a second which is completely represented by intermediate grey levels. The bright phase represents the magnetite and the dull grey phases are silica or silicates, with varying iron contents. This is corroborated by the iron and silicon X-Ray maps shown in Figures 4 and 5, which were generated by an electron-microprobe for the same magnification and section of specimen that produced the backscattered electron image in Figure 2. Clearly, the Taconite ore produces enough contrast for thresholding, and the magnetite can be easily discriminated from the gangue minerals. Thresholding, coupled with the fingerprinting procedure to eliminate artifacts and the usual phase filling procedure, complete the image processing stage. Areal fraction of phase was measured in each image, and the areal

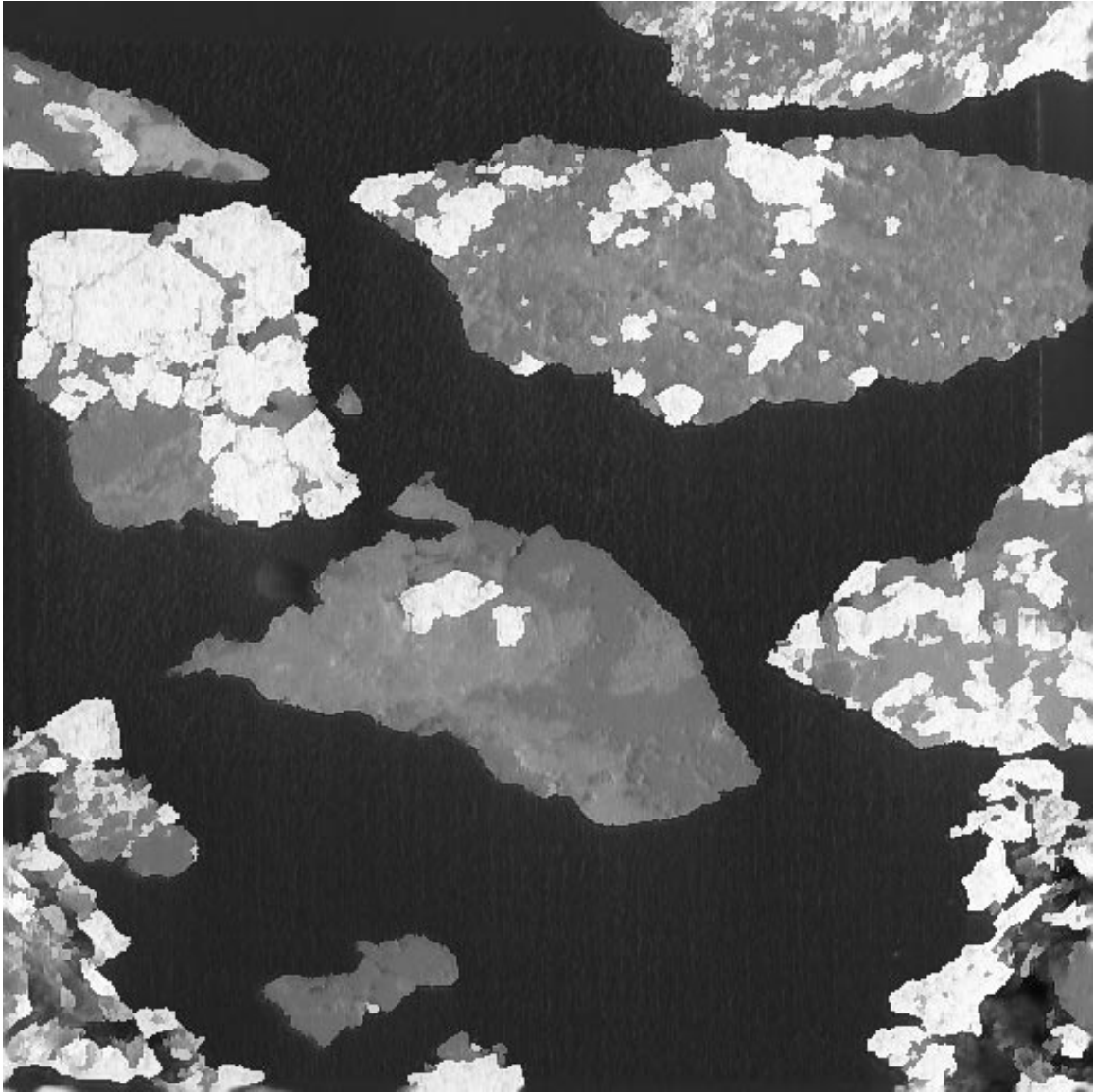


Figure 2 A backscattered electron image at 50X magnification of -500+355 micron particles from the Cyclone Underflow stream

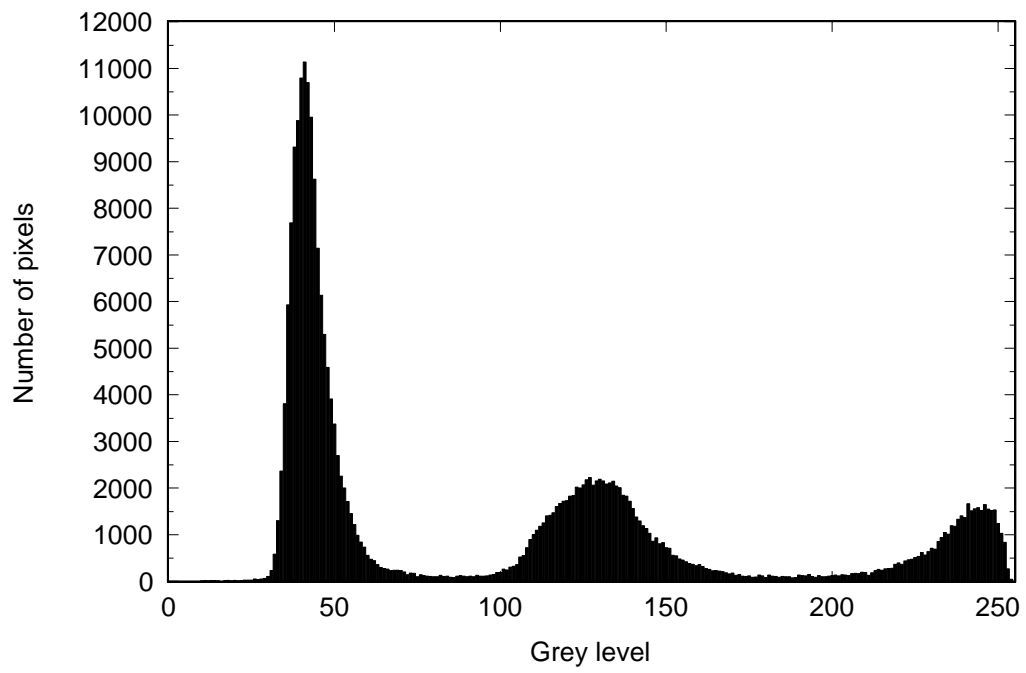


Figure 3 The grey level histogram corresponding to the image in Figure 5.2

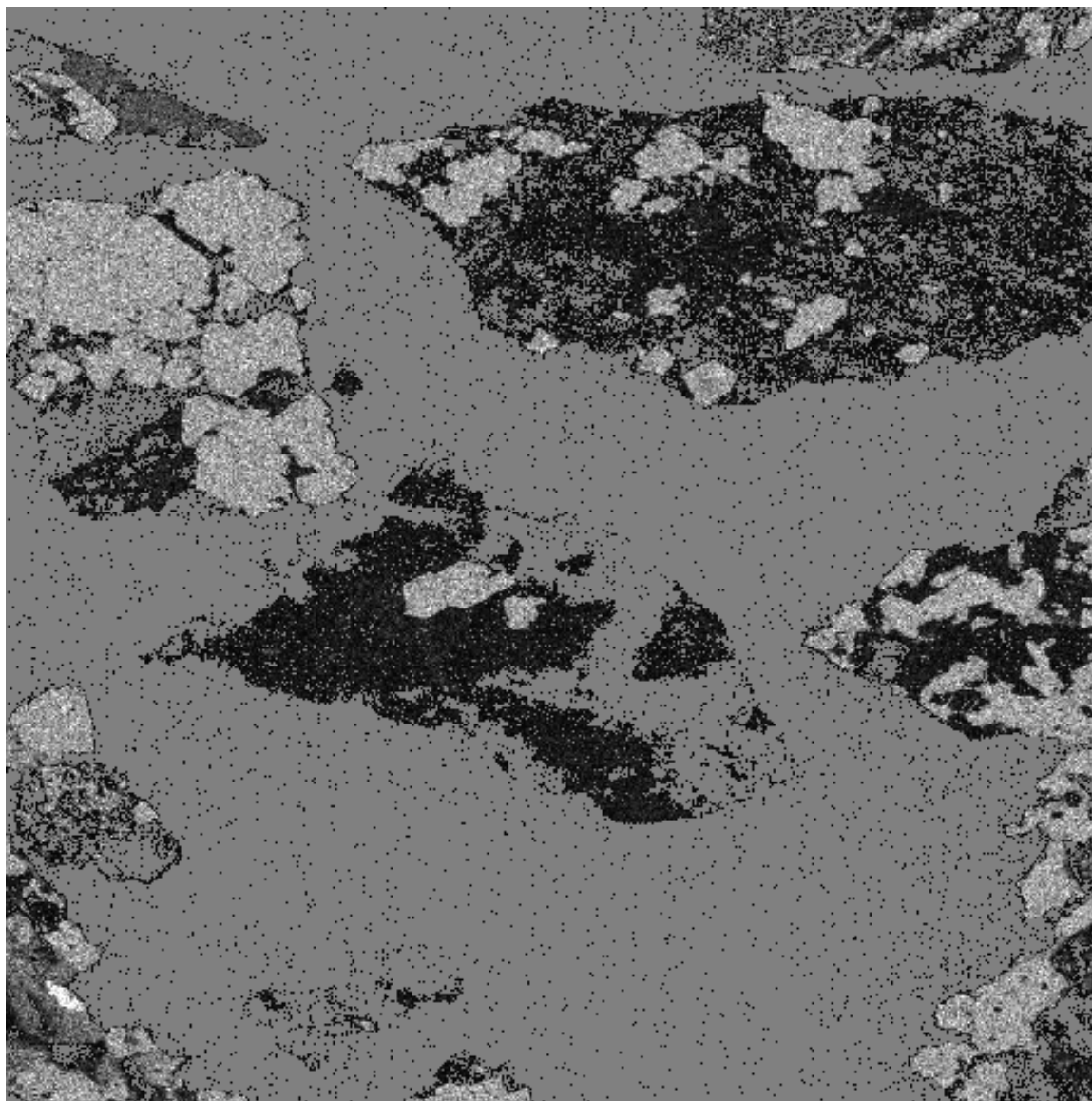


Figure 4 Iron X-Ray map corresponding to the image shown in Figure 5.2, scanned with an electron microprobe

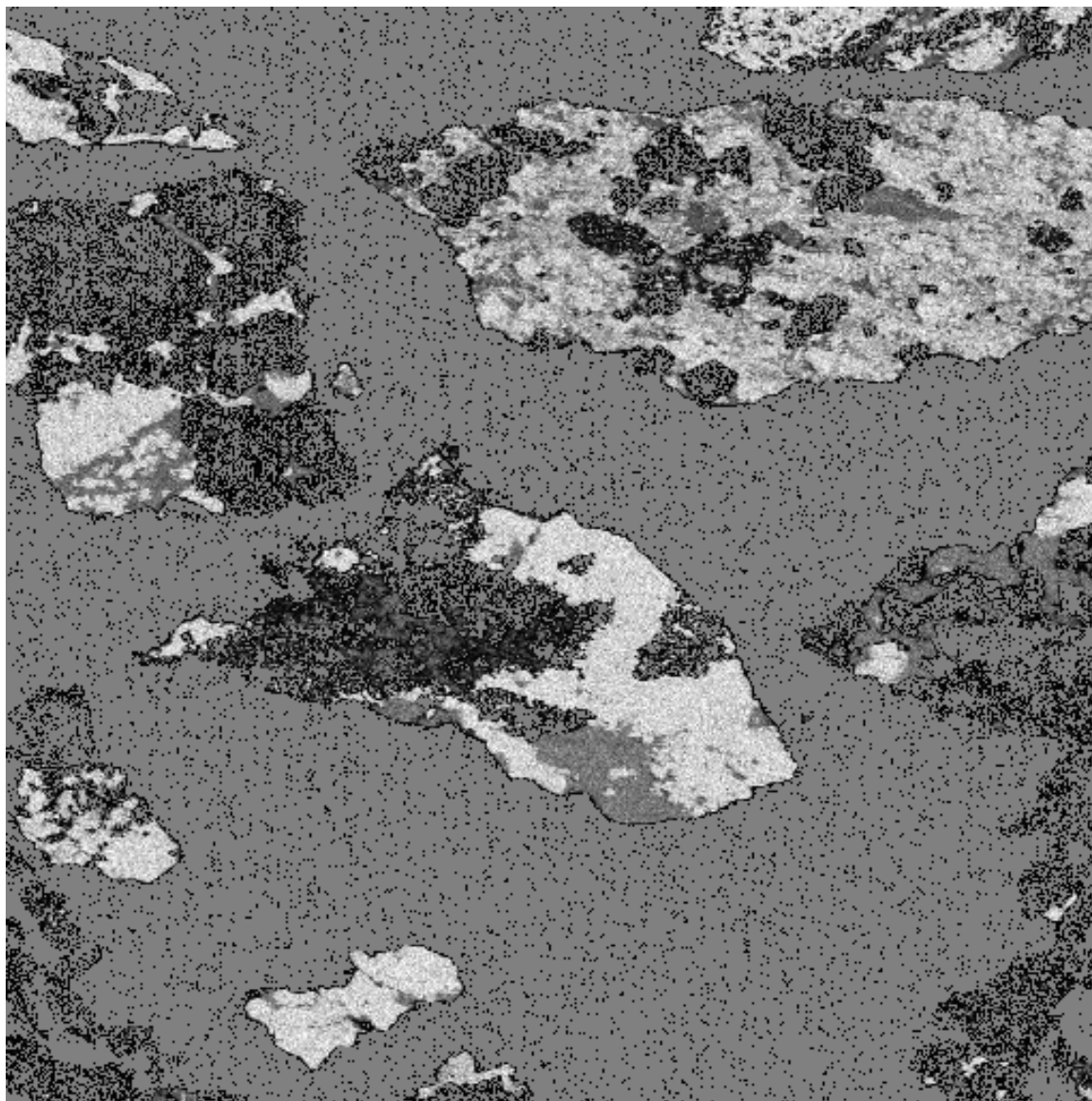


Figure 5 Silicon X-Ray map corresponding to the image shown in Figure 5.2, scanned with an electron microprobe

fraction of phase in each sample calculated. These were converted to grade fraction by weight using the measured densities of Chert and Magnetite that are reported in the experimental Phase and Texture Characterization section of this report. The measured grade of Magnetite in each sample is shown in Table 4. The total grade of Magnetite in each stream was calculated as the weighed average, with respect to the measured size distributions, of the grades in each size class. The results are also shown in Table 4.

The measurements of linear grade and chord length distributions were carried out using the same procedure used for the Dolomite-Sphalerite ore measurements. In Figure 6, a discriminated image from the -500+355 microns, Cyclone Underflow particles is shown at the standard 40X magnification. The measuring frame used for both, linear grade and chord length distributions, was 510 pixels. As shown in Figure 6, the chords that intercept the frame were not measured. The measured distributions were corrected for the probability that a chord intercepts the measuring frame. The linear grade and chord length distributions were measured in this fashion for every set of images acquired from each specimen corresponding to a narrow size sample from a given stream. The measured linear grade distributions by length corresponding to each sample are reported in the Appendix. These distributions must be retained for future use with the exact transformation kernel for stereological correction for the Taconite ore, when available. The character of this work may then be shifted from preliminary to definitive.

#### The Conditional, on size, Volumetric Grade Distributions

The linear grade distributions in the Appendix were used for calculation of the corresponding volumetric grade distributions using the symmetric transformation kernel

Table 4 Average grade as a function of size measured by image analysis

Size, microns		Fairlane Plant Grinding Circuit, Magnetite assays by image analysis, %									
Upper	Lower	B.M. Disch.	Cob. Conc.	Cyc. Feed	Cyc. Over	Cyc. Under	D.D. Conc.	D.D. Tails	Rough. Conc.	Rough. Tails	Scav. Conc.
1000	710	39.95	51.53	41.09	-	47.62	33.56	-	47.87	22.37	-
710	500	43.26	51.79	41.73	34.75	49.94	42.40	-	48.10	18.36	-
500	355	43.14	51.03	47.60	45.31	50.72	46.91	13.11	49.81	18.60	-
355	250	46.72	53.39	53.18	49.12	56.92	44.20	7.29	53.47	21.11	27.37
250	180	51.41	58.14	60.39	35.61	60.76	32.80	4.40	57.17	15.11	33.22
180	106	61.07	64.18	68.77	34.64	75.69	36.58	6.36	69.22	18.63	36.33
106	75	72.44	72.60	84.09	61.49	88.47	64.26	12.97	80.01	20.37	58.68
75	53	79.53	77.96	86.66	83.71	92.73	85.19	20.02	87.76	18.73	77.02
53	45	72.32	75.54	89.41	90.90	92.04	88.64	27.00	88.02	16.42	83.99
45	38	79.01	84.92	91.44	91.43	92.82	93.98	33.31	90.04	15.85	86.81
38	0	64.88	75.96	91.38	91.48	87.04	91.40	26.83	89.21	16.71	87.93
Average in stream		62.56	56.64	75.46	80.68	71.56	70.48	13.17	73.58	17.59	68.47

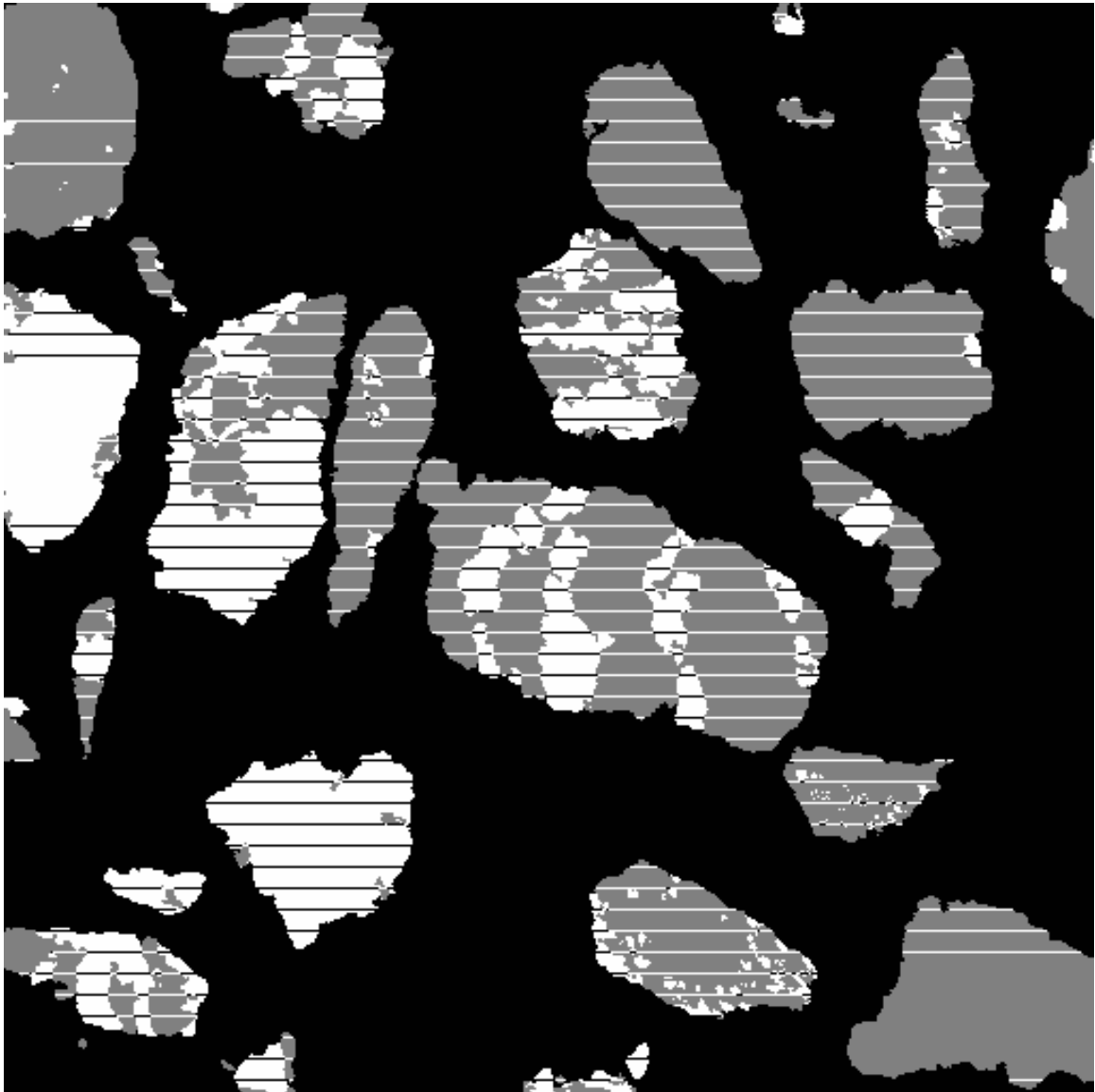


Figure 6 Discriminated image from -500+355 micron Cyclone Underflow particles at standard 40X magnification, and the measuring linear probes

developed from measurement on the Dolomite-Sphalerite ore and the stereological correction procedure in Schneider [2]. The volumetric grade distributions, weighted by volume, were converted to the corresponding volumetric grade distribution by weight, using the measured phase densities reported in the experimental Phase and Texture Characterization section that follows. These distributions are shown in Tables 5 through 14. Fortunately the texture of the Taconite ore is nearly symmetrical, and the symmetric transformation kernel can be used for the preliminary evaluation of the liberation characteristics of the ore. The volumetric grade distributions are fundamental in understanding the interactions between the textural characteristics of the ore and its liberation properties, as the particles interact with the unit operations in the various streams in the grinding circuit. The measured liberation spectra can be used to calibrate and model the unit operations in the circuit, i.e., Ball Mill, Hydrocyclones and Magnetic Drum separators.

#### Texture and Phase Characterization

Normally, the distributions used for modeling and simulation are in terms of particle grade, i.e., weight fraction of phase, and distributions by weight rather than volume. The conversion from volume to weight fractions is easily accomplished if the density of the phases is known. Furthermore, the liberation model requires, at the very least, a representative geometrical texture parameter, which describes the change in interphase area per unit volume of phase as particle composition changes. The representative geometrical texture parameter can be obtained by optimization, as described in Schneider [3], when the liberation spectra in the feed and product streams of a size

Table 5 The measured volumetric grade distributions, by weight, in the Ball Mill Discharge stream

Conditional, on size, volumetric grade distributions, weight % Size intervals in microns.											
volumetric grade interval, %	-1000 +710	-710 +500	-500 +355	-355 +250	-250 +180	-180 +106	-106 +75	-75 +53	-53 +45	-45 +38	-38
0	0.00	0.00	0.12	0.0	0.17	0.00	0.00	7.11	12.79	12.91	29.24
0 - 10	0.10	0.10	2.89	6.71	13.45	9.97	15.34	4.45	10.33	2.10	0.09
10 - 20	19.58	0.32	16.27	8.55	3.46	6.22	0.95	4.32	0.15	1.97	2.19
20 - 30	56.97	62.46	16.34	38.91	31.83	7.85	4.02	0.00	1.76	0.00	0.07
30 - 40	22.54	34.40	63.29	15.82	10.18	26.46	5.95	3.82	3.26	2.00	0.90
40 - 50	0.06	1.99	0.69	19.04	11.78	3.49	0.52	0.08	0.09	0.78	0.04
50 - 60	0.14	0.13	0.16	10.55	9.46	5.34	4.56	0.09	0.09	0.61	0.09
60 - 70	0.15	0.14	0.06	0.11	12.66	3.48	5.86	0.09	0.10	1.73	0.58
70 - 80	0.16	0.16	0.00	0.16	5.59	7.63	14.27	0.55	3.03	2.07	0.61
80 - 90	0.15	0.14	0.13	0.15	1.23	29.36	22.86	16.39	13.71	12.37	30.97
90 - 100	0.15	0.15	0.05	0.00	0.19	0.22	25.18	63.05	54.68	48.74	11.88
100	0.00	0.00	0.00	0.00	0.00	0.00	0.48	0.05	0.01	14.72	23.34

Table 6 The measured volumetric grade distributions, by weight, in the Cobber Concentrate stream

Conditional, on size, volumetric grade distributions, weight % Size intervals in microns.											
volumetric grade interval, %	-1000 +710	-710 +500	-500 +355	-355 +250	-250 +180	-180 +106	-106 +75	-75 +53	-53 +45	-45 +38	-38
0	0.00	0.00	0.08	0.00	0.00	0.41	5.12	7.34	6.51	2.45	14.13
0 - 10	0.09	0.09	0.01	3.54	11.94	10.86	7.97	4.18	8.00	6.59	4.08
10 - 20	1.08	0.03	2.44	6.68	3.01	5.98	4.60	4.87	6.77	2.97	3.04
20 - 30	26.62	25.86	45.49	22.42	12.25	8.83	6.69	4.32	5.20	0.00	0.00
30 - 40	45.84	58.60	20.53	31.95	19.88	9.26	3.84	0.35	0.02	0.14	1.19
40 - 50	24.98	7.48	23.94	14.83	18.09	12.22	0.00	0.95	0.00	0.38	0.00
50 - 60	1.13	7.59	3.92	13.69	4.25	5.53	0.41	0.06	0.05	0.17	0.03
60 - 70	0.11	0.20	3.55	6.56	5.86	5.28	0.17	0.07	0.05	0.83	0.09
70 - 80	0.02	0.06	0.01	0.29	8.26	9.49	8.76	0.00	0.48	2.84	0.00
80 - 90	0.07	0.09	0.00	0.03	16.37	25.95	26.27	26.01	13.68	10.31	12.58
90 - 100	0.05	0.00	0.00	0.00	0.08	6.19	36.16	51.06	59.21	61.08	60.87
100	0.01	0.00	0.02	0.00	0.00	0.00	0.00	0.79	0.01	12.24	4.00

Table 7 The measured volumetric grade distributions, by weight, in the Cyclone Feed stream

Conditional, on size, volumetric grade distributions, weight % Size intervals in microns.											
volumetric grade interval, %	-1000 +710	-710 +500	-500 +355	-355 +250	-250 +180	-180 +106	-106 +75	-75 +53	-53 +45	-45 +38	-38
0	0.00	0.00	0.00	0.00	0.00	1.29	1.38	0.41	1.30	0.39	3.61
0 - 10	0.10	0.10	0.09	0.09	6.32	2.63	0.93	2.64	1.89	3.34	0.00
10 - 20	1.21	13.78	0.80	12.37	2.89	2.75	3.29	3.26	1.74	0.00	0.26
20 - 30	77.23	53.32	48.34	10.52	14.31	18.24	2.02	2.64	2.08	2.06	1.70
30 - 40	20.36	32.17	40.81	42.58	21.45	5.55	1.35	0.42	0.26	0.40	1.06
40 - 50	0.39	0.15	9.11	14.77	11.26	6.15	5.21	0.87	0.55	0.43	0.08
50 - 60	0.14	0.11	0.26	16.27	12.15	5.53	3.27	0.00	0.40	1.15	0.08
60 - 70	0.14	0.00	0.34	1.36	17.26	15.36	2.30	6.26	0.00	0.10	0.09
70 - 80	0.14	0.07	0.10	1.71	2.85	11.15	10.40	4.83	0.15	2.50	3.74
80 - 90	0.14	0.13	0.00	0.14	10.57	26.36	31.67	21.60	26.33	0.17	2.78
90 - 100	0.15	0.18	0.00	0.18	0.93	5.00	31.22	56.02	61.76	77.06	55.35
100	0.00	0.00	0.14	0.00	0.00	0.01	6.99	1.04	3.55	12.40	31.25

Table 8 The measured volumetric grade distributions, by weight, in the Cyclone Overflow stream

Conditional, on size, volumetric grade distributions, weight % Size intervals in microns.											
volumetric grade interval, %	-1000 +710	-710 +500	-500 +355	-355 +250	-250 +180	-180 +106	-106 +75	-75 +53	-53 +45	-45 +38	-38
0	-	0.00	0.00	0.00	0.00	2.76	5.38	3.51	1.25	0.68	3.59
0 - 10	-	0.10	2.98	3.62	20.08	21.28	1.19	2.58	1.83	2.90	0.00
10 - 20	-	29.92	9.29	4.65	24.96	31.33	18.53	1.51	0.99	1.14	0.01
20 - 30	-	61.15	16.31	31.04	7.20	0.88	4.39	3.69	0.15	0.92	0.03
30 - 40	-	7.94	63.03	33.11	47.15	37.59	13.86	2.68	1.18	1.41	2.42
40 - 50	-	0.14	6.19	15.65	0.18	5.60	9.71	1.17	0.79	0.94	0.08
50 - 60	-	0.14	1.64	10.65	0.22	0.00	2.47	0.09	0.59	0.65	0.29
60 - 70	-	0.15	0.21	1.00	0.05	0.00	1.01	1.77	0.09	1.24	1.98
70 - 80	-	0.15	0.13	0.20	0.08	0.02	4.76	7.55	0.00	0.85	1.28
80 - 90	-	0.15	0.00	0.08	0.00	0.00	28.48	21.33	21.79	6.39	13.05
90 - 100	-	0.16	0.22	0.00	0.08	0.13	10.21	54.12	55.98	28.40	41.94
100	-	0.00	0.00	0.00	0.00	0.40	0.00	0.01	15.37	54.49	35.32

Table 9 The measured volumetric grade distributions, by weight, in the Cyclone Underflow stream

Conditional, on size, volumetric grade distributions, weight % Size intervals in microns.											
volumetric grade interval, %	-1000 +710	-710 +500	-500 +355	-355 +250	-250 +180	-180 +106	-106 +75	-75 +53	-53 +45	-45 +38	-38
0	0.00	0.00	0.08	0.00	0.00	0.00	0.00	0.00	0.00	0.59	6.28
0 - 10	0.10	0.09	0.01	0.09	5.82	0.08	0.28	0.14	0.75	1.45	1.21
10 - 20	0.43	0.38	0.35	0.93	0.01	0.05	2.14	3.11	2.82	1.46	2.30
20 - 30	44.44	18.21	40.14	29.64	12.48	7.78	1.97	0.83	0.61	0.25	0.38
30 - 40	54.20	75.74	44.49	19.97	29.61	11.28	3.31	1.17	0.87	0.24	0.08
40 - 50	0.12	2.78	1.27	28.03	3.91	12.91	0.18	0.41	0.12	0.81	0.08
50 - 60	0.13	2.42	12.51	6.76	17.46	8.19	1.66	0.18	1.60	0.28	0.09
60 - 70	0.14	0.16	0.96	5.13	14.43	17.82	2.25	0.08	0.79	0.09	0.09
70 - 80	0.15	0.16	0.20	5.58	9.01	0.03	4.72	0.20	2.38	1.08	2.76
80 - 90	0.14	0.00	0.00	3.80	6.49	22.77	32.60	2.09	12.18	15.22	13.32
90 - 100	0.15	0.00	0.00	0.07	0.79	19.10	50.90	85.16	66.70	45.42	48.61
100	0.00	0.06	0.00	0.00	0.00	0.00	0.01	6.64	11.16	33.11	24.80

Table 10 The measured volumetric grade distributions, by weight, in the Dewatering Drum Concentrate stream

Conditional, on size, volumetric grade distributions, weight %											
Size intervals in microns.											
volumetric grade interval, %	-1000 +710	-710 +500	-500 +355	-355 +250	-250 +180	-180 +106	-106 +75	-75 +53	-53 +45	-45 +38	-38
0	0.03	0.00	0.03	0.00	0.96	0.01	4.52	1.35	0.53	0.24	3.18
0 - 10	0.08	0.10	0.07	5.53	21.18	15.00	5.30	3.12	0.21	0.39	0.00
10 - 20	32.53	6.73	3.92	5.22	22.64	31.47	4.96	1.31	4.70	0.45	0.60
20 - 30	65.47	58.90	38.12	39.32	43.58	24.95	8.27	6.01	1.08	1.55	0.00
30 - 40	1.01	32.35	48.76	39.76	9.31	22.93	4.19	2.06	1.54	1.93	0.15
40 - 50	0.13	1.18	8.55	9.59	1.69	4.81	24.41	2.00	3.92	0.18	0.12
50 - 60	0.14	0.14	0.09	0.00	0.41	0.05	4.72	0.00	1.53	0.08	0.09
60 - 70	0.15	0.15	0.16	0.22	0.15	0.00	5.14	0.03	1.58	0.04	0.35
70 - 80	0.15	0.16	0.14	0.29	0.07	0.00	6.22	4.40	2.04	0.28	0.21
80 - 90	0.15	0.14	0.16	0.06	0.00	0.03	23.30	19.88	2.57	16.35	18.40
90 - 100	0.16	0.15	0.00	0.00	0.01	0.01	8.98	48.22	80.18	42.73	56.85
100	0.00	0.00	0.00	0.00	0.00	0.74	0.00	11.62	0.13	35.79	20.06

Table 11 The measured volumetric grade distributions, by weight, in the Dewatering Drum Tails stream

Conditional, on size, volumetric grade distributions, weight %											
Size intervals in microns.											
volumetric grade interval, %	-1000 +710	-710 +500	-500 +355	-355 +250	-250 +180	-180 +106	-106 +75	-75 +53	-53 +45	-45 +38	-38
0	-	-	6.77	63.71	69.25	70.86	39.51	35.22	36.85	25.32	67.92
0 - 10	-	-	70.12	12.95	24.27	14.59	27.77	27.00	29.91	34.28	0.20
10 - 20	-	-	21.63	21.93	4.80	10.48	23.75	20.73	0.86	9.24	3.05
20 - 30	-	-	0.37	0.26	0.60	2.92	7.52	0.70	8.63	1.00	0.36
30 - 40	-	-	0.14	0.14	0.10	0.14	0.00	2.35	1.64	1.34	0.53
40 - 50	-	-	0.15	0.15	0.52	0.15	0.76	7.11	3.05	1.16	0.07
50 - 60	-	-	0.16	0.16	0.31	0.17	0.14	2.07	0.80	1.85	0.51
60 - 70	-	-	0.16	0.16	0.00	0.16	0.11	0.29	3.29	1.64	0.53
70 - 80	-	-	0.17	0.17	0.11	0.17	0.10	4.44	5.69	5.38	4.62
80 - 90	-	-	0.17	0.17	0.00	0.17	0.17	0.03	7.63	10.45	16.00
90 - 100	-	-	0.18	0.18	0.03	0.18	0.18	0.00	1.65	8.34	6.21
100	-	-	0.00	0.00	0.00	0.00	0.00	0.07	0.00	0.00	0.00

Table 12 The measured volumetric grade distributions, by weight, in the Rougher Concentrate stream

Conditional, on size, volumetric grade distributions, weight %											
Size intervals in microns.											
volumetric grade interval, %	-1000 +710	-710 +500	-500 +355	-355 +250	-250 +180	-180 +106	-106 +75	-75 +53	-53 +45	-45 +38	-38
0	0.00	0.00	0.00	0.00	0.00	0.00	1.09	0.61	1.96	1.57	2.67
0 - 10	0.10	0.10	0.10	0.09	9.40	6.07	2.91	2.49	1.96	2.27	2.07
10 - 20	0.56	1.09	1.04	0.26	3.81	4.44	3.72	0.20	1.39	1.74	2.31
20 - 30	24.13	44.65	42.02	34.49	11.36	8.68	7.48	3.54	3.08	0.84	0.00
30 - 40	73.72	47.83	35.91	21.77	21.25	10.14	5.95	1.30	3.65	0.30	0.02
40 - 50	0.99	3.93	13.42	25.41	26.83	1.69	3.23	5.31	0.00	0.40	0.14
50 - 60	0.21	2.03	6.55	16.96	5.36	6.06	2.63	0.08	0.09	2.48	0.26
60 - 70	0.00	0.20	0.59	0.58	8.62	12.77	0.81	0.08	0.10	1.01	1.27
70 - 80	0.03	0.08	0.17	0.15	4.97	28.09	3.05	0.23	0.23	1.38	2.62
80 - 90	0.11	0.10	0.09	0.16	5.00	21.86	20.50	25.87	18.37	8.95	7.97
90 - 100	0.16	0.00	0.11	0.14	3.40	0.16	48.62	55.91	55.36	52.98	79.09
100	0.00	0.00	0.00	0.00	0.00	0.04	0.01	4.38	13.81	26.07	1.57

Table 13 The measured volumetric grade distributions, by weight, in the Rougher Tails stream

Conditional, on size, volumetric grade distributions, weight % Size intervals in microns.											
volumetric grade interval, %	-1000 +710	-710 +500	-500 +355	-355 +250	-250 +180	-180 +106	-106 +75	-75 +53	-53 +45	-45 +38	-38
0	0.41	0.00	4.87	8.23	43.71	27.63	27.78	47.50	49.58	67.49	69.80
0 - 10	20.58	52.87	57.82	32.07	18.86	29.32	40.04	22.53	33.88	14.56	10.06
10 - 20	77.74	35.92	14.18	50.70	26.30	27.15	8.34	8.98	2.43	4.37	2.06
20 - 30	0.64	10.02	21.80	7.27	8.07	3.60	17.40	11.03	1.06	0.42	0.71
30 - 40	0.01	0.27	0.53	0.78	2.09	10.26	0.00	0.41	0.90	1.54	2.22
40 - 50	0.03	0.14	0.02	0.14	0.15	0.52	0.02	0.13	1.04	0.00	0.12
50 - 60	0.00	0.14	0.25	0.15	0.16	0.12	0.01	0.14	1.62	1.02	0.13
60 - 70	0.13	0.15	0.18	0.17	0.16	0.04	0.05	0.15	1.12	1.24	2.22
70 - 80	0.15	0.15	0.20	0.15	0.16	0.33	0.04	3.33	1.53	2.25	0.83
80 - 90	0.15	0.16	0.15	0.16	0.17	0.42	0.02	0.98	2.70	3.26	7.37
90 - 100	0.16	0.17	0.00	0.17	0.18	0.00	1.56	0.30	4.13	3.63	4.48
100	0.00	0.00	0.00	0.00	0.00	0.00	4.75	4.53	0.00	0.23	0.00

Table 14 The measured volumetric grade distributions, by weight, in the Scavenger Concentrate stream

Conditional, on size, volumetric grade distributions, weight % Size intervals in microns.											
volumetric grade interval, %	-1000 +710	-710 +500	-500 +355	-355 +250	-250 +180	-180 +106	-106 +75	-75 +53	-53 +45	-45 +38	-38
0	-	-	-	0.00	0.00	0.09	3.55	5.04	5.65	0.51	4.05
0 - 10	-	-	-	32.11	17.89	26.07	16.56	3.47	0.76	6.10	3.75
10 - 20	-	-	-	32.96	38.90	32.89	4.50	4.97	3.33	3.44	0.84
20 - 30	-	-	-	34.05	19.03	14.04	10.87	4.18	4.20	0.00	0.07
30 - 40	-	-	-	0.35	19.91	11.83	11.12	6.11	1.66	2.09	0.66
40 - 50	-	-	-	0.05	2.98	0.47	7.54	0.53	0.05	0.21	0.88
50 - 60	-	-	-	0.00	0.65	2.22	4.27	0.53	0.54	0.27	0.08
60 - 70	-	-	-	0.04	0.09	2.82	4.27	2.01	0.08	0.19	0.99
70 - 80	-	-	-	0.13	0.00	2.92	3.56	7.68	0.66	1.61	0.20
80 - 90	-	-	-	0.15	0.16	6.63	13.11	23.99	9.20	8.01	13.99
90 - 100	-	-	-	0.16	0.16	0.00	20.63	41.48	73.87	76.72	49.73
100	-	-	-	0.00	0.23	0.00	0.00	0.00	0.00	0.84	24.77

reduction operation are known. However, it is not yet possible to measure the parameter  $\phi_r$  directly from the ore. Also, the dependency of texture on particle size is not yet understood. The value of the parameter  $\phi$  at a given particle size can be measured directly from the ore by image analysis, from particles in narrow size and narrow grade intervals like the ones produced here. Narrow size particles are easily obtained by screening. However, particle samples in narrow grade intervals require some fractionation procedure. The Taconite ore is not suitable for magnetic fluid fractionation, due to the strong ferromagnetism of the magnetite. The fractionation procedure used here is the standard heavy liquid fractionation, using organic liquids and a 125 ml separation funnel. A sample of the -710+500 microns Ball Mill Discharge weighing 56.8 g was prepared for dense liquid fractionation. The heavy liquids used were Tetrabromoethane,  $\rho = 2.954$  g/cc, and Diodomethane,  $\rho = 3.325$  g/cc. Diodomethane diluted with Triethyl Orthophosphate was used to give a separation density at  $\rho = 3.112$  g/cc. After fractionation, the particles were weighed and their average density measured in a helium pycnometer. The fractionation results are shown in Table 15. Each sample was mounted, ground and polished, as previously described. A set of 40 images per specimen was collected, and the images were processed also as previously described. In Figures 7, 8, 9 and 10, backscattered electron images selected arbitrarily from each set corresponding to a narrow grade interval are shown. Again, the dull grey phase represents Silicates and the bright phase represents Iron Oxides. The images show very graphically the increased contribution of Iron Oxides as particle density increases. Few liberated particle cross sections are observed, which indicates that fractionation was successful. In Table 15,

Table 15 Dense liquid fractionation of -710+500 microns Ball Mill Discharge particles

Separation density, g/cc	Weight fraction, %	Average density, g/cc Helium pycnometer	Volumetric grade, % Image Analysis
-2.954	21.65	2.870	5.67
-3.112 +2.954	12.32	3.092	11.94
-3.325 +3.112	13.56	3.284	18.73
+3.325	52.47	4.009	51.24

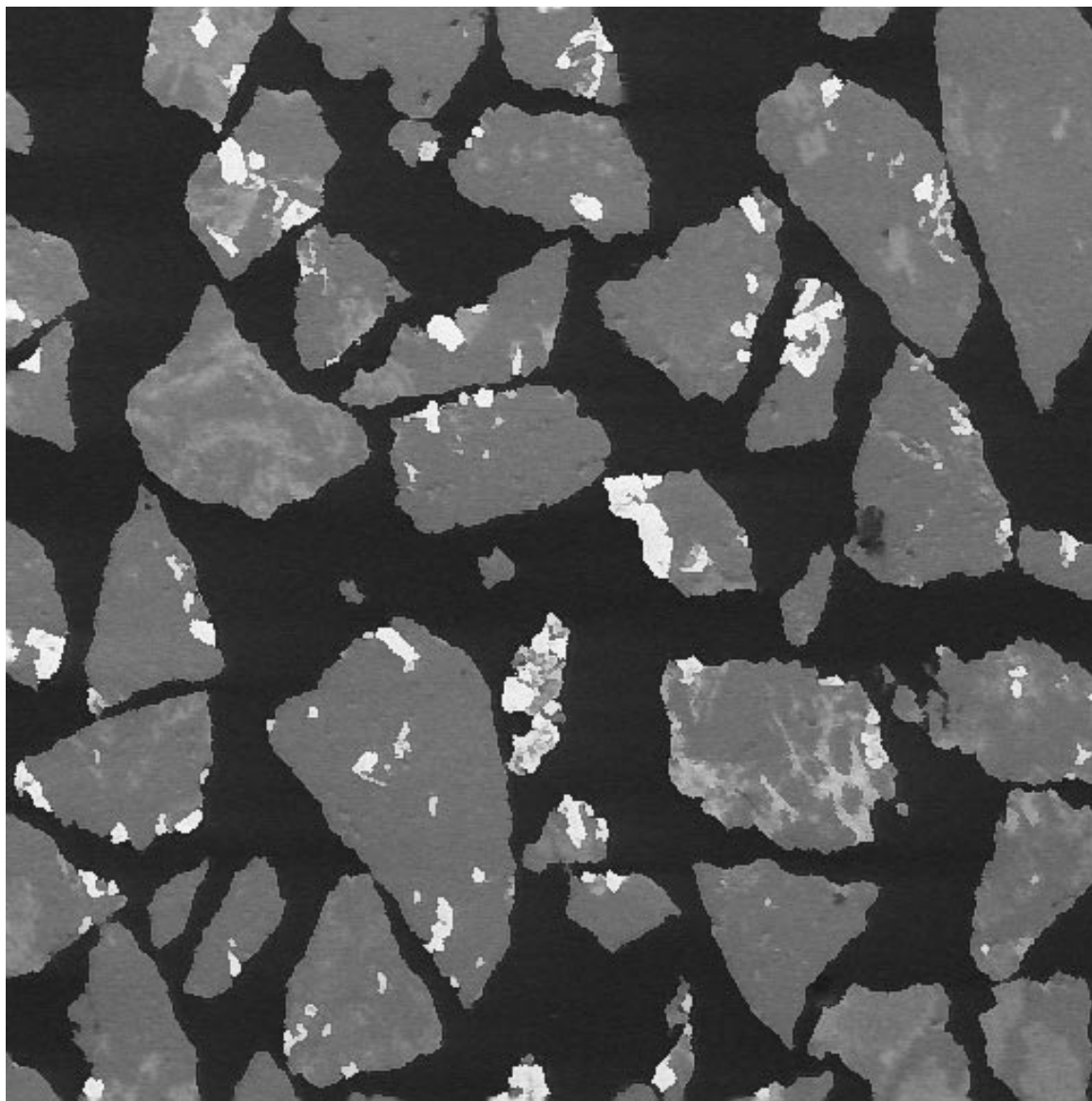


Figure 7 Backscattered electron image from -710+500 micron, -2.954 g/cc fractionated particles

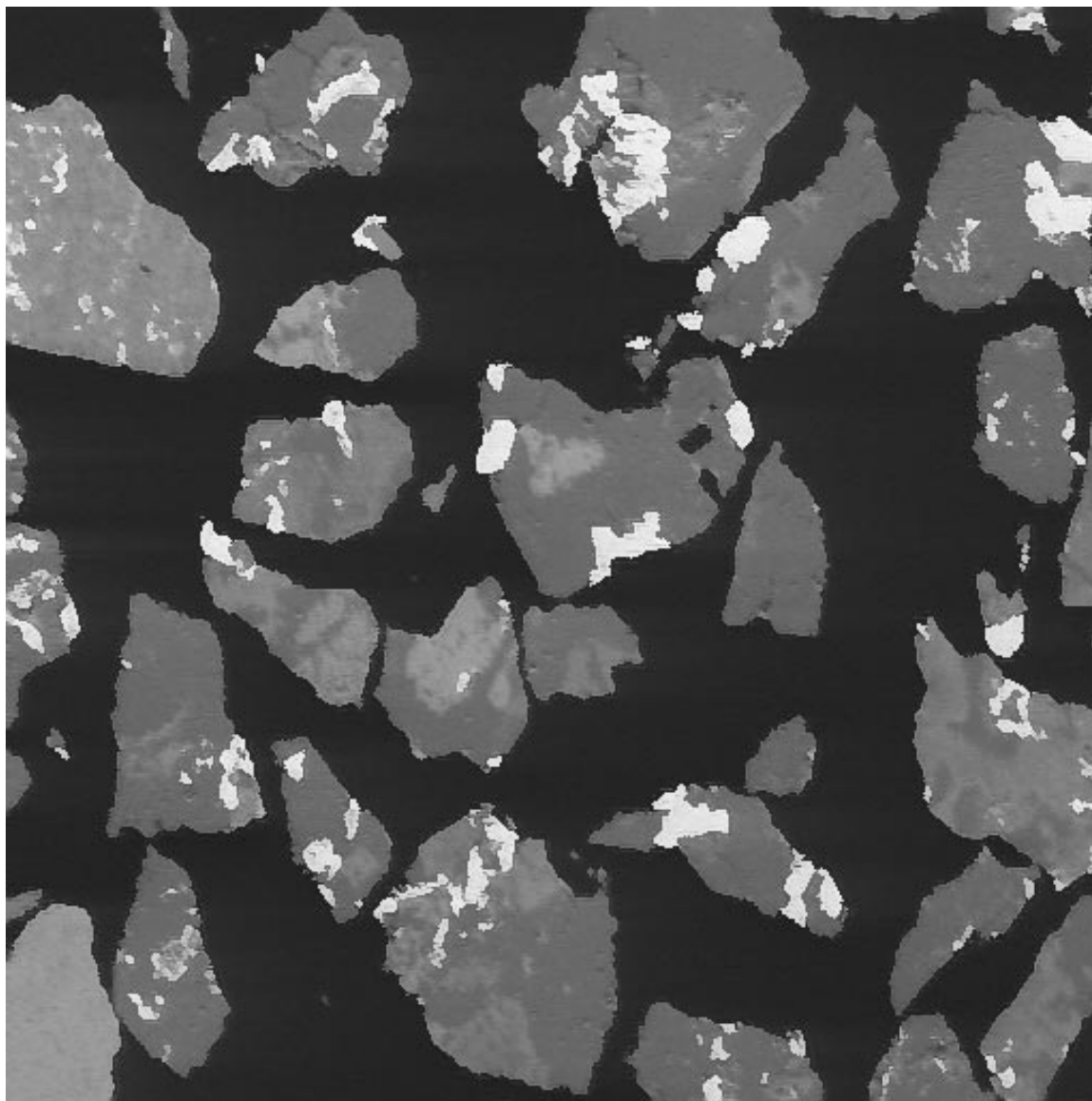


Figure 8 Backscattered electron image from -710+500 micron, -3.112+2.954 g/cc fractionated particles

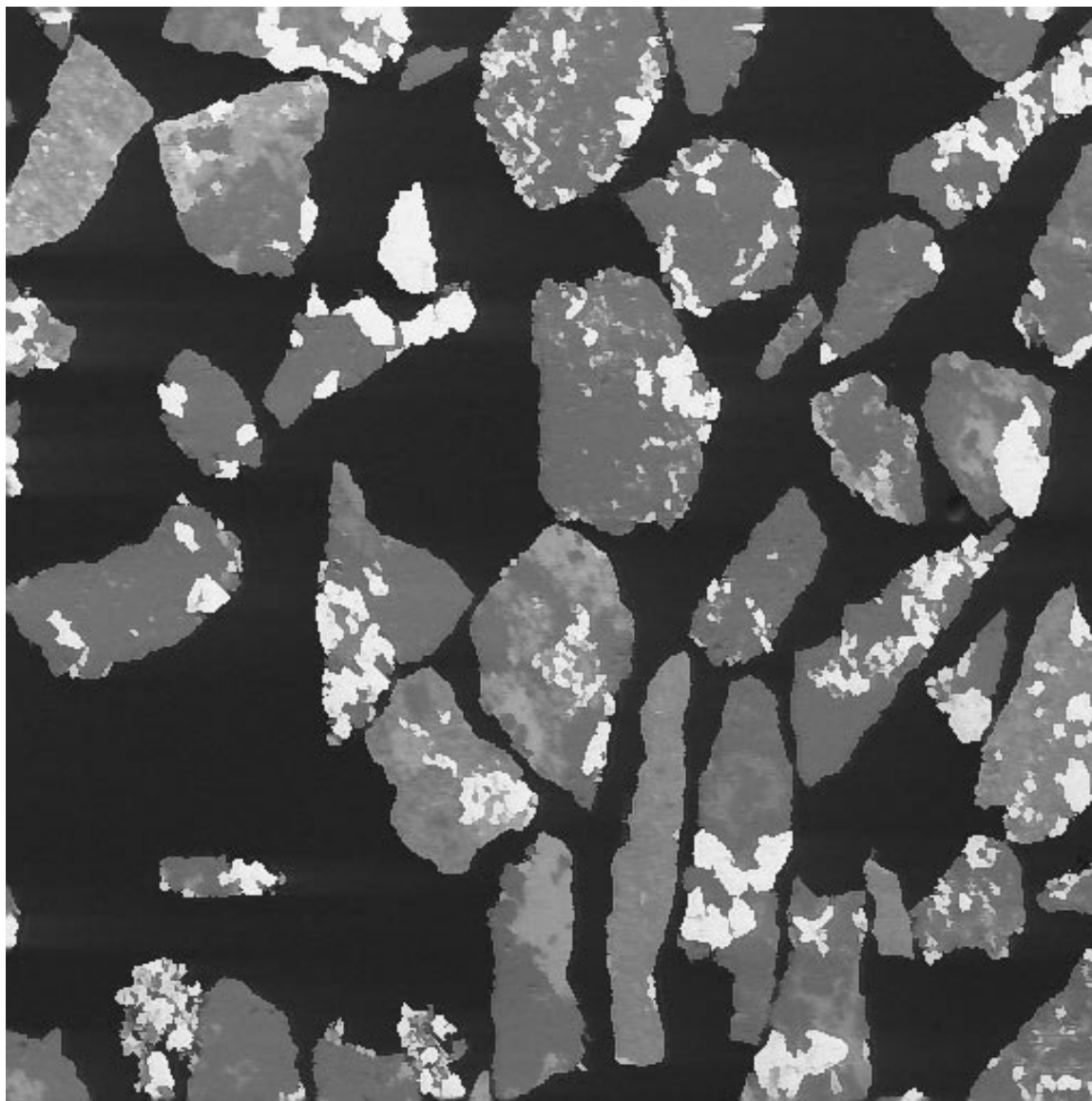


Figure 9 Backscattered electron image from -710+500 micron, -3.325+3.112 g/cc fractionated particles

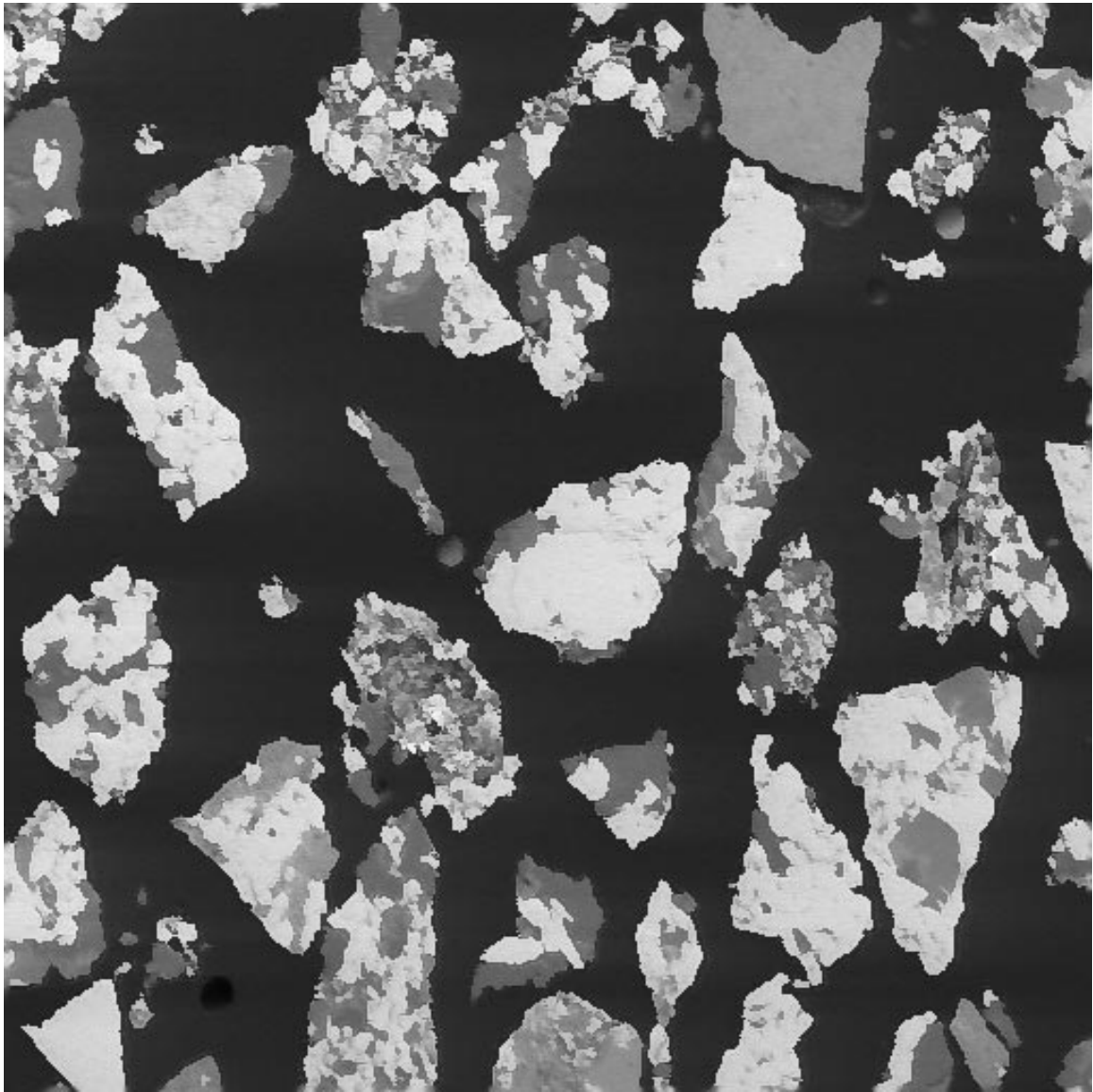


Figure 10 Backscattered electron image from -710+500 micron, +3.325 g/cc fractionated particles

the measured volumetric grade of each fractionated sample is reported. If we denominate as phase A all the silicates present, mainly Chert, and phase B all iron oxides, mainly Magnetite, the densities of phases A and B can be calculated by plotting the fractionated sample densities, as measured by pycnometry, against the corresponding volumetric grade as measured by image analysis. This is shown in Figure 11. The straight line indicates that the ore is essentially binary with respect to density. In Figure 11, the density of phases A and B are calculated from the intercept and the slope of the line that fits the measured points. Linear regression yields  $\rho_A = 2.761 \text{ g/cc}$  and  $\rho_B = 5.378 \text{ g/cc}$ , completing the phase characterization procedure.

Since the particles were already fractionated for phase density determination, it is possible to use the images to measure the value of the textural parameter  $\phi$  at this size range. For this, the average chord length for both phases and features was measured from the fractionated particle sample specimens. The average chord lengths were used to calculate the surface area per unit volume of both phases and the features as well. With these values, the interphase area per unit volume of phase  $S_{vAB}$  and  $S_{vBA}$  could be calculated. The results are shown in Table 16. The geometrical texture parameter  $\phi(-710+500\mu)$ , is calculated by plotting the product of representative particle size and interphase area per unit volume of phase against the volumetric grade of the corresponding phase. Here, the representative particle size is  $d_p = \sqrt{D_{upper} D_{lower}} = 595.82 \text{ microns}$ . The resulting plot is shown in Figure 12, and linear regression yields  $\phi(-710+500\mu) = 45.06$ .

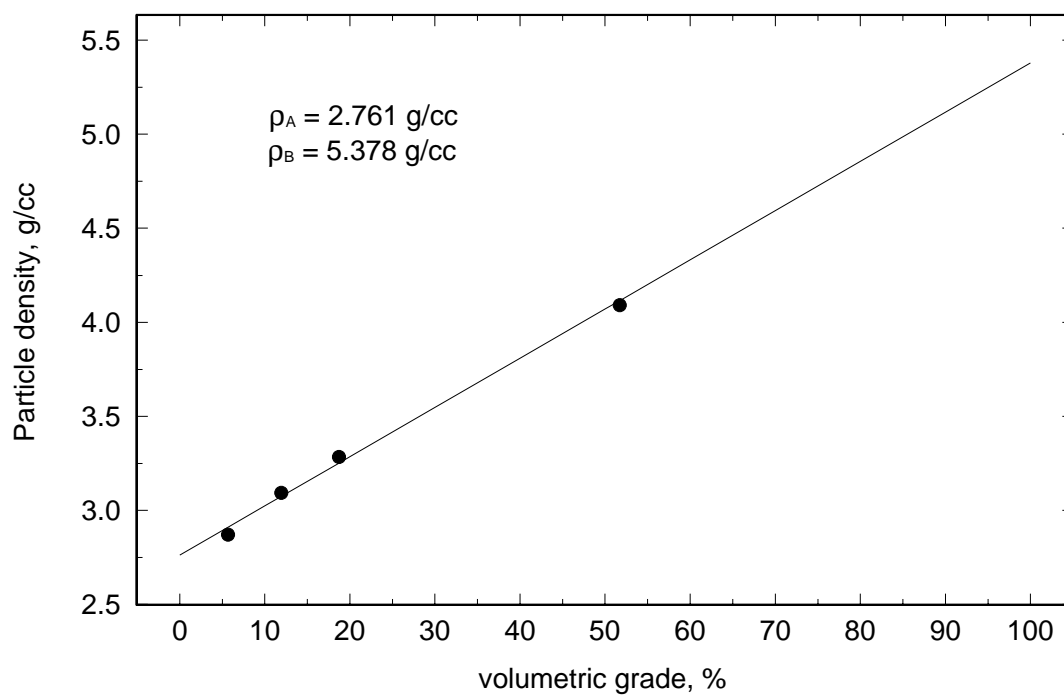


Figure 11 Correlation between average sample density by Helium Pycnometry and average sample volumetric grade by image analysis, and phase density determination

Table 16 The interphase area per unit volume of phase and the corresponding volumetric grades measured on the narrow size, narrow grade samples from fractionation

Density range, g/cc	Volumetric grade of phase A, Silicates	Interphase area per unit volume of phase A	Volumetric grade of phase B, Iron Oxides	Interphase area per unit volume of phase B
-2.954	0.9433	$4.371 \times 10^{-3}$	0.0567	$7.289 \times 10^{-2}$
-3.112 +2.954	0.8806	$8.667 \times 10^{-3}$	0.1194	$6.337 \times 10^{-2}$
-3.325 +3.112	0.8127	$1.544 \times 10^{-3}$	0.1873	$6.622 \times 10^{-2}$
+3.325	0.4876	$3.621 \times 10^{-3}$	0.5124	$3.380 \times 10^{-2}$

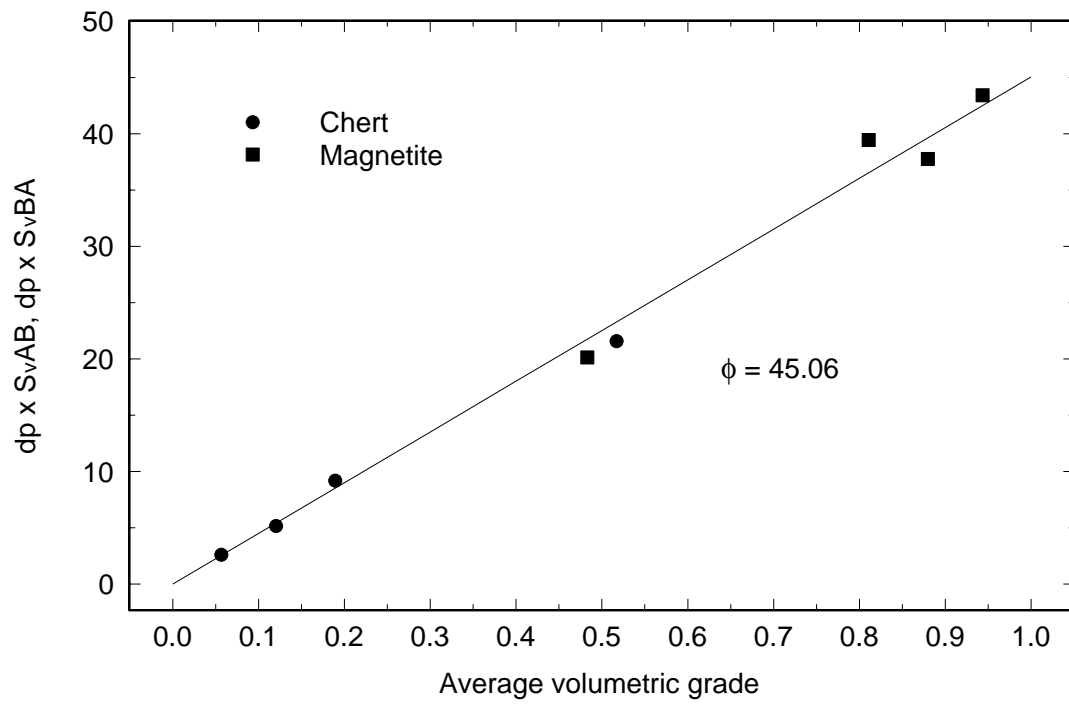


Figure 12 Taconite ore geometrical texture parameter determination

## **MODSIM Simulation Setup and Models**

The flowsheet setup for the simulation of the secondary grinding circuit is shown in Figure 13. The main feed stream is the Cobber Concentrate. The Dewatering Drum magnetic separation was regarded as a subsidiary separation unit, and the concentrate and tails streams were treated as secondary feed streams to the main circuit, with constant size and liberation spectra. The Scavenger Concentrate stream was also treated as a subsidiary feed stream with constant size and liberation spectra.

The size distributions in the four feed streams were entered in MODSIM as shown in Table 2. The conditional liberation spectra were entered as measured for all available sizes in the feed streams. For the larger size fractions, where the liberation spectra was not measured either because there were not enough particles available for image analysis or because of the 1000 microns top size limitation for the *I.A.* system used, the liberation spectrum measured on the largest size sample was repeated. This assumption is significant only for the Cobber Concentrate stream, which contains approximately 47% of particles larger than 1000 microns. The measured, conditional on size, liberation spectra corresponding to the Cobber Concentrate stream is shown in Figure 14. It is clear from the figure that the particles at the larger size classes, approaching the 1000 microns top size, are very closely distributed around the volumetric grade corresponding to the volumetric abundance of Magnetite in the stream. Clearly, this behavior must be retained for particles larger than 1000 microns, and the assumption of constant liberation spectra above 1000 microns for the Taconite particles in the Cobber Concentrate stream is not expected to produce significant error in the circuit simulation.

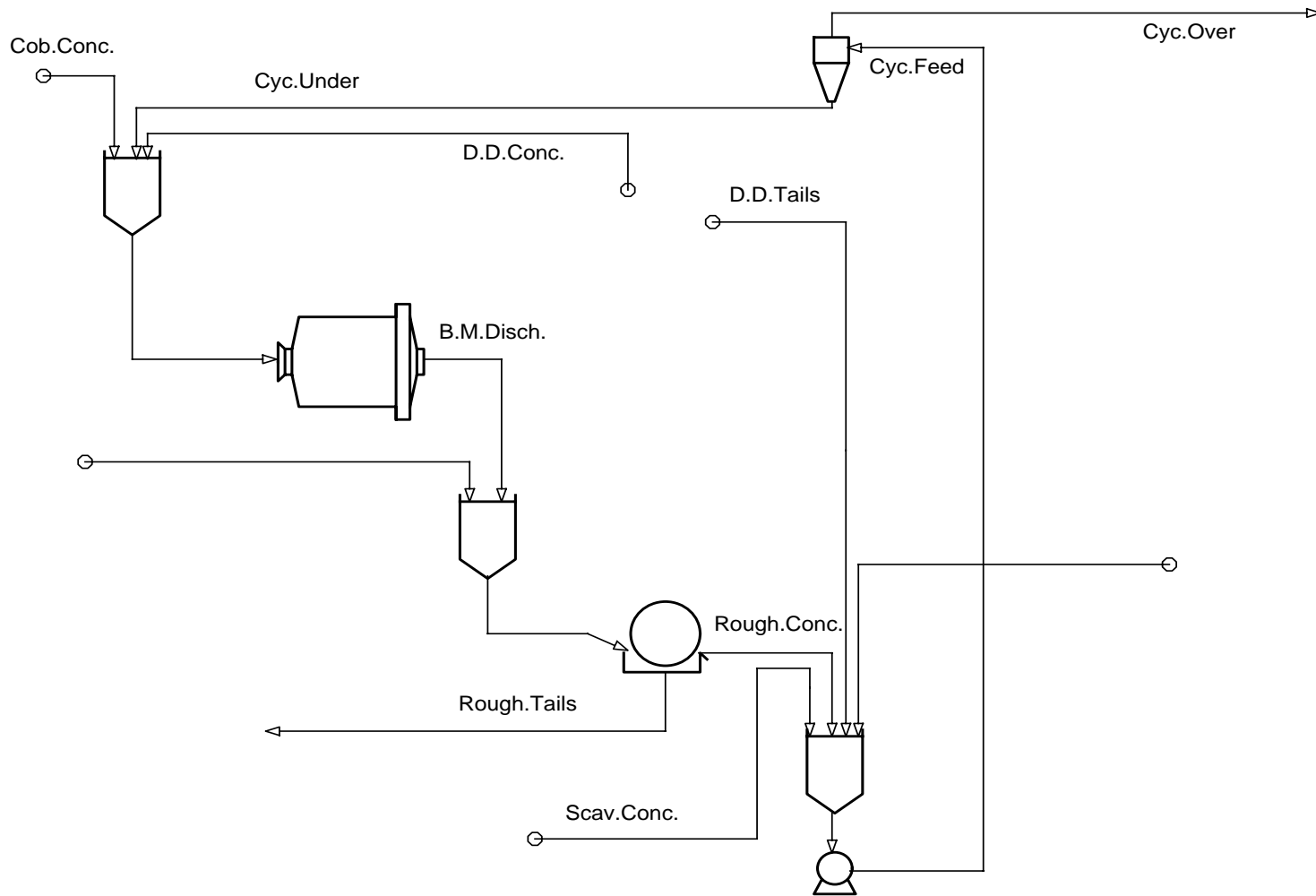


Figure 13 The flowsheet used in MODSIM for the simulation of the Fairlane secondary grinding circuit

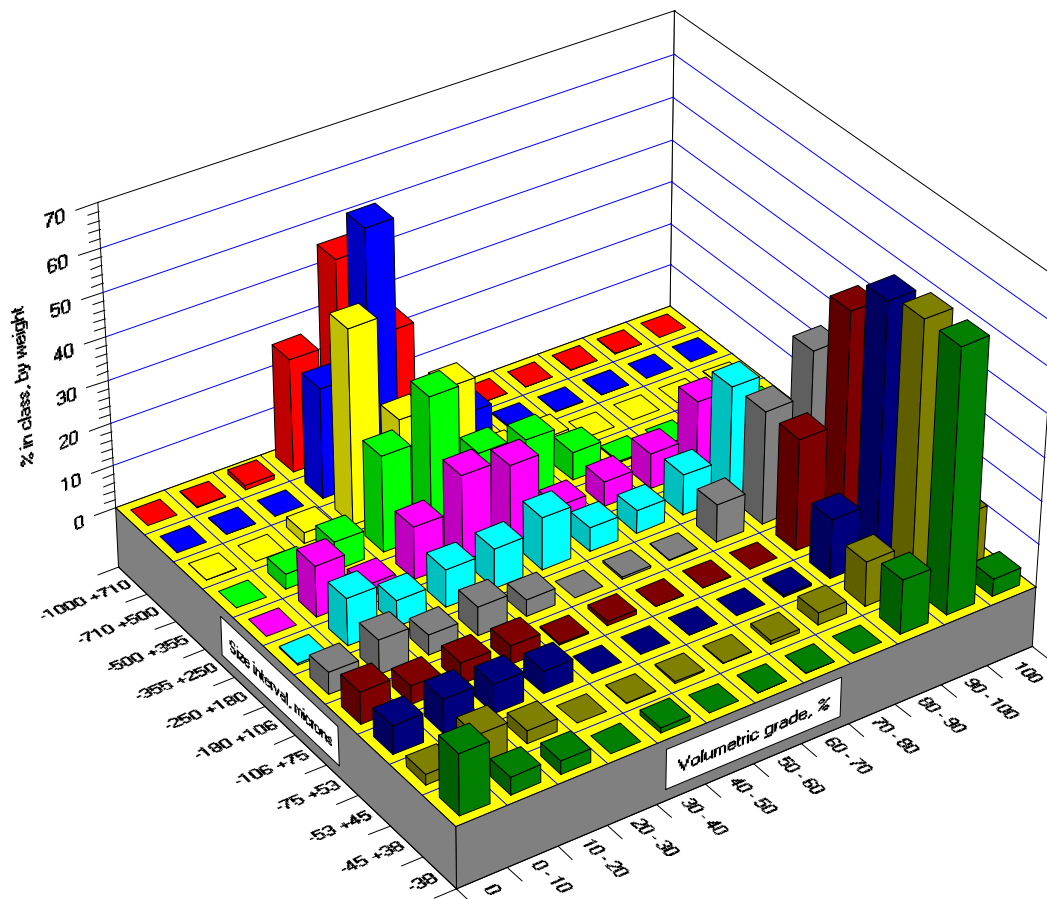


Figure 14 The measured, conditional on size, liberation spectra in the Cobber Concentrate stream

The primary objectives of the simulation were to match the plant's nominal material balance, as shown in Table 17, and to match the measured size and liberation spectra in each stream. The solids feed rates entered in the simulator were equal to the nominal feed rates obtained from the plant's material balance. Water feed rates were calculated by MODSIM so that the nominal solids content in each feed stream in the circuit were reproduced. The simulation of the secondary grinding circuit requires, besides the liberation model, a comminution model for the ball mill and concentration/classification models for both the rougher wet magnetic drum separator and the hydrocyclone. The models were adjusted and the best set of parameters was obtained by both independent optimization of each unit operation, and manually by repeated simulation of the entire circuit.

#### Liberation Model

The liberation model was used as described in Schneider [4], with modifications to the critical parameters  $\phi_A^C$  and  $\phi_B^C$ , the variance parameter  $\zeta$  and the shape of the variance function, and to the shape of the boundary of the accessible region associated with phase *B*. The modifications are due to the peculiarities of the textural properties of the Taconite ore, in contrast with the Dolomite-Sphalerite ore texture.

The critical texture parameters were set at  $\phi_A^C = 25.0$  and  $\phi_B^C = 9.00$  with respect to a representative geometrical texture parameter  $\phi_r$  set equal to the measured geometrical texture parameter  $\phi(-710+500\mu)$  as shown in Figure 12, i.e.,  $\phi_r = 45.0$ . This clearly indicates that the Chert starts liberating at considerably larger sizes than the Magnetite.

The composite particles of Taconite seem to shift, upon breakage, from

Table 17 The nominal flow rates and % solids and the measured grades in the streams of the secondary grinding circuit of the Fairlane Plant. Recoveries are based on the total flow rates from the four feed streams. Stream grades are calculated from image analysis results in each size range and the measured/adjusted size distributions

Stream	Solid Flow, Tons/hour	Water Flow, m <sup>3</sup> /hour	solids, %	Recovery of solids, %	Recovery of Chert, %	Grade of Chert, %	Recovery of Magnetite, %	Grade of Magnetite, %
Cob.Conc.	301.26	137.89	68.60	79.11	83.09	43.36	76.32	56.64
Cyc.Feed	618.37	474.35	56.59	162.39	96.52	24.54	208.71	75.46
Cyc.Under	381.77	64.69	85.51	100.26	69.06	28.44	122.19	71.56
Cyc.Over	236.60	679.39	25.83	62.13	29.08	19.32	85.54	80.68
D.D.Conc.	57.48	30.34	65.45	15.09	10.79	29.52	18.12	70.48
D.D.Tails	4.82	59.36	7.51	1.27	2.66	86.83	0.28	13.17
B.M.Disch.	740.51	230.14	76.29	194.47	176.35	37.44	207.20	62.56
Rough.Conc.	618.57	526.93	54.00	162.44	103.95	26.42	203.57	73.58
Rough.Tails	121.94	1913.79	5.99	32.02	63.92	82.41	9.59	17.59
Scav.Conc.	17.23	23.50	42.30	4.52	3.46	31.53	5.28	68.47

intermediate volumetric grade classes to the volumetric grade classes corresponding to nearly liberated particles rather quicker than the composite particles of Dolomite-Sphalerite. Yet, once they reach the nearly liberated state, the particles liberation rate is comparatively slow. It is interesting to note that the liberation behavior of a binary ore can be viewed under opposite perspectives. With respect to the Taconite ore, one could say that, upon breakage, composite particles generate a very small fraction of progeny in the intermediate grade classes. One could also say that particles in the intermediate grade classes tend to change their liberation state faster than particles in nearly liberated grade classes, which tend to retain their liberation state.

The behavior of the Taconite particles is not well described by the Dolomite-Sphalerite model functional form for the variance, as described in Schneider [4], and for the Taconite ore, it was found that the following functional form was considerably more effective:

$$\sigma_{\xi}^2 = \begin{cases} \frac{\zeta}{2} \frac{g_v'}{0.3} (n_{1\xi}^B - n_{1\xi}^{B2}) & g_v' \leq 0.3 \\ \frac{\zeta}{2} (n_{1\xi}^B - n_{1\xi}^{B2}) & 0.3 < g_v' < 0.8 \\ \frac{\zeta}{2} \frac{(1 - g_v')}{0.2} (n_{1\xi}^B - n_{1\xi}^{B2}) & 0.8 \leq g_v' \end{cases} \quad (1)$$

with the variance parameter set at  $\zeta = 1.95$ . In Equation 1, variance is maximum and constant for particles with volumetric grades between 0.3 and 0.8. The variance is null for liberated particles and varies linearly with parent volumetric grade when parent

volumetric grade is smaller than 0.3 or higher than 0.8.

The modified variance model for the Taconite ore works best in conjunction with the following modification to the shape of the boundary of the accessible region associated to phase B:

$$g_v^{B,Taconite} = \begin{cases} g_v^B & g_v^B < 1, g_v' \leq 0.3 \\ \frac{(1+g_v^B)}{2} & g_v^B < 1, 0.3 < g_v' < 0.8 \\ g_v^B & g_v^B < 1, 0.8 \leq g_v' \end{cases} \quad (2)$$

where  $g_v^B$  is defined as in Schneider [4], for the Dolomite-Sphalerite texture. Equation 2 allows for a broader range of grades in which progeny from intermediate grade particles can be produced, relative to the Dolomite-Sphalerite model. However, care was taken so that the limiting bounds of the accessible region for phase B became active when and if violated by the boundary defined by Equation 2.

The modifications to the liberation model defined in Equations 1 and 2 are in fact a rough adjustment to the Dolomite-Sphalerite model such that the liberation characteristics of the Taconite ore are better reproduced when simulating the Taconite grinding circuit in this study. The modifications were made exclusively by comparing simulated and measured liberation spectra. More important than the modifications in themselves is the fact that they were necessary, and consequently indicating that the texture of a particular ore, depending on its peculiarities, may require modifications to the boundary models and to the variance model, in addition to reparameterization.

## Comminution Model

There is no information on the particle size distribution in the holdup of the ball mill at the Fairlane Plant. Consequently, classification effects in the mill with respect to particle size cannot be accessed. In fact, the ball mill feed stream was not sampled for particle size distribution measurement. The only direct information available, besides some operational conditions, and the mill's geometry, that is useful for the choice and parameterization of the comminution model, is the size distribution in the product stream. The feed stream to the ball mill could not be sampled due to the plant's physical configuration. A priori, only an approximate size distribution in the feed stream should be sufficient for a preliminary parameterization work. This was obtained by adding the measured size distributions in the Cobber Concentrate, Cyclone Underflow, and Dewatering Drum Concentrate streams, and using the nominal material balance in Table 17. Since the size distribution in the product is not very sensitive to the size distribution in the feed, an approximate distribution should be enough to choose the proper comminution model and to obtain an initial set of parameters by independent optimization.

It was assumed that the transport in the mill can be described by three perfectly mixed regions in series, with the fractional residence times for the solids shown in Schneider [3]. This assumption is probably inaccurate, particularly when considering the geometry of the ball mill, which has a diameter to length ratio of approximately 1:2.5. However, this assumption has no impact whatsoever at this stage of the investigation, and the only direct consequence is that the parameters for the model equations corresponding

to the selection and breakage functions become even more alienated to the comminution properties of the ore from the phenomenological point of view.

The three mixers in series with post-classification model is described in Schneider [3]. When classification is not considered, the classification coefficients  $C_i$  are null for every particle size  $i$ , and consequently  $p_i = p_i^* = p_i^{(3)}$  and  $\tau_3' = \tau_3$ . The breakage function model chosen for the Taconite ore was Austin's [5] three parameter normalizable function, as shown in Schneider [3]. The selection function for the Taconite ore was modeled by:

$$S_i = S_1 \left( \frac{d_{pi}}{1000} \right)^\alpha \quad (3)$$

It is interesting to point out that the best model for the selection function did not require a description for an abnormal breakage region, perhaps due to the comparatively small particle sizes in the mill's feed. The final parameters for the comminution model of the ball mill are shown in Table 18, including breakage function and selection function parameters, and the residence times in the mill.

#### Wet Magnetic Drum Separator Model

The model developed for the Rougher separation was empirical, in nature. The classification action in a wet magnetic drum separator is primarily a function of the volumetric abundance of the magnetic phase, here the Magnetite, in the particle. In practice, because the separators are simple drums that produce a constant magnetic field and that rotate at constant speed, the configuration of the feed streams and how the

Table 18 The comminution model parameters for the ball mill used in MODSIM simulation

Selection function parameters	$\alpha = 1.28855$ $S_1 = 1.28076 \text{ min}^{-1}$
Breakage function parameters	$\Phi = 0.46085$ $\beta = 0.44601$ $\gamma = 0.98684$
Average residence time in perfectly mixed region $n$ (minutes)	$\tau_1 = 0.0548$ $\tau_2 = 0.8492$ $\tau_3 = 3.0960$
Total residence time (minutes)	$\tau = 4.0$

particles are exposed to the magnetic field, is of crucial importance. Here, at least at this preliminary modeling stage, it is considerably more important to establish a classification function that can be used to model the classification action, with respect to both particle size and grade, of the magnetic separator.

The classification phenomenon in the unit can be described by:

$$c(g_v, d_p) = \alpha(d_p) + (1 - \alpha(d_p)) e(g_v) \quad (4)$$

where  $c(g_v, d_p)$  represents the fraction of particles that have volumetric grade  $g_v$  and representative size  $d_p$  that report to the tails stream. The by-pass fraction of particles in the feed that short circuits to the tails stream is represented by  $\alpha(d_p)$ , which is only a function of particle size. The primary classification function, represented by  $e(g_v)$ , is exclusively dependent on particle composition.

The by-pass function  $\alpha(d_p)$  is based on the principle that smaller particles are more susceptible to the drag produced by the water flow. Approximately 80% of the water in the feed of the Rougher separator reports to the tails stream (Table 17), and some water drag must be expected. The by-pass function was modeled by:

$$\alpha(d_p) = \kappa e^{-\zeta d_p} \quad (5.5)$$

where  $\kappa$  and  $\zeta$  are arbitrary model parameters.

The classification function  $e(g_v)$  was modeled with the commonly used Rosin-Rammler functional form:

$$e(g_v) = 1 - e^{-0.693 \left( \frac{1 - g_v}{1 - g_v^{50}} \right)^\lambda} \quad (5.6)$$

where  $g_v^{50}$  represents the volumetric grade of a particle that have equal probability of reporting either to the concentrate or to the tail streams and  $\lambda$  is related to the separation sharpness index  $SI$ , defined by  $SI = \frac{g_v^{25}}{g_v^{75}}$ . For the Rosin-Rammler functional form, this is:

$$SI = e^{-\frac{1.5725}{\lambda}} \quad (5.7)$$

The following set of parameters were used for the Rougher separation in MODSIM, using the model for a wet magnetic drum separator described above:

- Sharpness Index,  $SI = 0.8926$
- Separation volumetric grade,  $g_v^{50} = 0.090$
- By-pass fraction,  $\kappa = 0.466$
- Exponential factor to reduce by-pass as particle size increases,  $\zeta = 56.00 \text{ m}^{-1}$

Finally, the water split factor to the tails stream was set to 0.784, completing the modeling of the Rougher separation unit.

#### Hydrocyclone Classification Model

The Hydrocyclone is the most common classification operation used in industrial grinding circuits. Consequently, the classification action in hydrocyclones has been the subject of a large number of studies. The most sophisticated hydrocyclone models are based on solutions to the Navier-Stokes transport equations, in two dimensions, [6] and most recently, a considerable effort has been made by Cortes [7], towards the three dimensional solution. However, these models are rather complex, and at this time, their

implementation in a MODSIM like simulator is not yet feasible. The alternatives are first, the use of models based on correlation studies, as for example Lynch's model [8] and Plitt's model [9], and second, the use of empirical classification models. The correlation models are implemented with advantage, since these models allow some flexibility at simulating the effect of changes in operational conditions of the hydrocyclone, and its geometry. The sampling campaign at the Fairlane Plant produced enough data, with respect to geometry and operational conditions, for the implementation of a correlation based model, and this should be pursued once this study takes on the plant's performance optimization character. At this initial stage, when the liberation characteristics of the Taconite ore and the liberation model are under evaluation, it is more appropriate to select a simpler, fewer parameters empirical classification model.

Empirical classification models have been used by Schneider [3] for modeling of an elutriation operation, and in the previously described modeling of the wet magnetic drum separator. Here, this modeling technique is once again employed to describe the hydrocyclone operation at the Fairlane Plant. For a general description of empirical models for classification operations the interested reader is referred to King [10]. The classification action in the hydrocyclone can be described by:

$$c(d_p, g_v) = \alpha + (1 - \alpha) e(d_p, g_v) \quad (5.8)$$

where  $e(d_p, g_v)$  is called the corrected classification function and  $c(d_p, g_v)$  is called the actual classification function. The parameter  $\alpha$  represents the fraction of particles that by-passes to the underflow stream, and here this is constant with respect to both particle size and composition. The corrected classification function was modeled with the logistic

functional form:

$$e(d_p, g_v) = \frac{1}{1 + \left( \frac{d_p}{d_p^{50}(g_v)} \right)^{-\lambda}} \quad (5.9)$$

where the exponential parameter  $\lambda$  is related to the separation sharpness index  $SI$  by:

$$SI = e^{-\frac{2.1972}{\lambda}} \quad (5.10)$$

and  $d_p^{50}(g_v)$  represents the separation size for a particle that has composition  $g_v$ . The change in separation size with particle composition was modeled by:

$$d_p^{50}(g_v) = d_{50} \left( \frac{\rho_A}{\rho(g_v)} \right)^\delta \quad (5.11)$$

In equation 11, the strong concentration action in the hydrocyclone operation due to differential particle density is taken into account, and the value of the parameter  $m$  is related to the flow regime in the device, with the lower limit of 0.5 corresponding to laminar flow conditions, and higher values for turbulent flow [10].

Equations 8 through 11 represent a typical empirical model that can be used to describe the classification action, with respect to size and composition, in mineral processing devices, when liberation information is available.

The following set of parameters were used for the hydrocyclone classification in MODSIM, using the empirical model described above:

- Sharpness Index,  $SI = 0.6058$
- Separation size,  $d_{50} = 123.0$  microns
- Exponential parameter in separation size function,  $\delta = 0.8$
- By-pass fraction,  $\alpha = 0.0865$

Finally, the water split to the underflow stream was assumed to be equal to the by-pass fraction  $\alpha$ , completing the preliminary hydrocyclone modeling.

### **MODSIM Simulation Results**

The objective of the simulation is primarily to reproduce, to the greatest accuracy, the measured size and grade distributions in the plant. There are six streams in the circuit for which measured and simulated results are available, namely the Ball Mill Discharge, the Rougher Concentrate and the Rougher Tails streams, around the Rougher magnetic separator node, and the Cyclone Feed, Underflow and Overflow streams, around the Hydrocyclone node. The simulated size distributions in the streams above are compared to the adjusted size distributions (Table 3), which represent measured data, in Figure 15. There is excellent agreement between simulated and measured size distributions in every stream, with the exception of the Rougher Tails stream, which could not be fully reproduced by simulation. The measured size distribution in the Rougher Tails stream is considerably finer than the corresponding simulated size distribution. It is possible that the smallest particles were favored during sampling, either due to the awkward sampling point, located under the magnetic separators at a difficult point to reach from the plant's floor, or due to the relatively high water flow rate in the stream and its low solids content (Tables 17 and 1). Actually, the Rougher Tails stream contains the least solids and

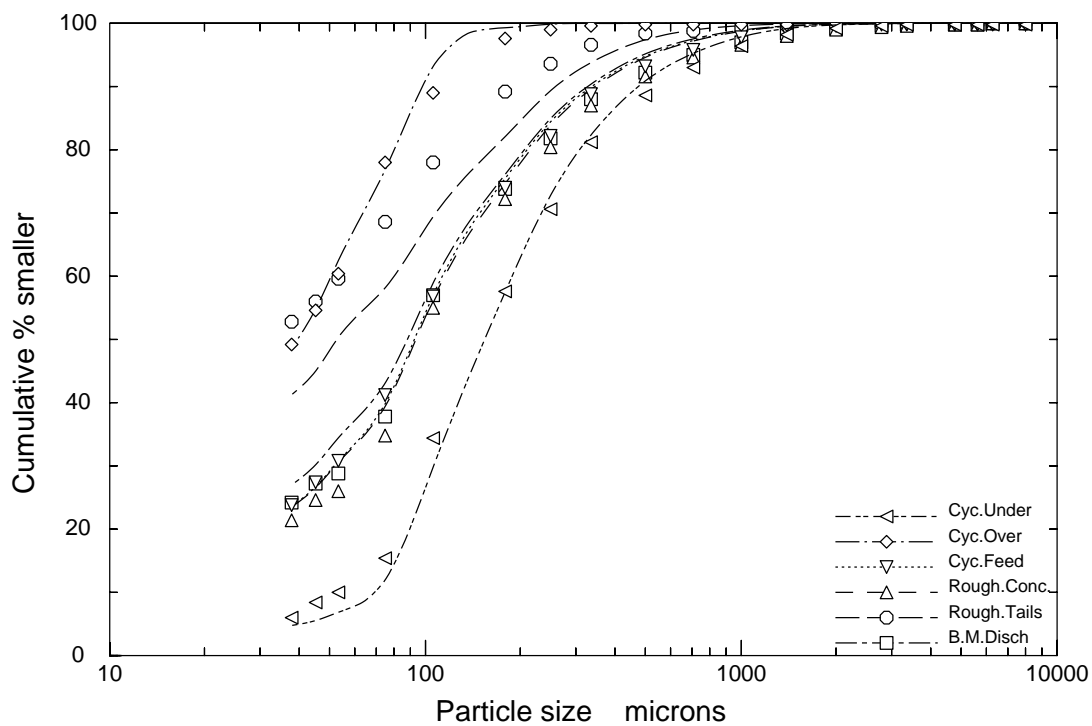


Figure 14 Comparison between measured and simulated size distributions in the Fairlane Plant secondary grinding circuit. Points show measured distributions and lines show calculated distributions

the highest water flow rate in the circuit, which makes it the most difficult stream to sample accurately. However, it is very important to point out that if the stream had not been analyzed for its grade distribution, it would be possible to match the measured size distribution by simulation almost perfectly. This is because the grade distributions impose a tight constraint to the parameterization of the unit operations, and consequently the simulation becomes considerably more realistic, and any sampling error more apparent.

The measured and simulated composite grade distributions around the Rougher magnetic separator and the Hydrocyclone are shown in Figure 16, and the simulation results show very good agreement with the measured data. The plots in Figure 16 represent the result of the entire effort put forward in order to measure and characterize the liberation properties of the Taconite ore. The immediate conclusion is that it is possible to simulate this grinding circuit fairly accurately, with respect to both liberation and comminution properties, using the procedures described in this work. Moreover, it is now possible to use the simulator to investigate the configuration of the plant with respect to its performance.

Finally, the simulated material balance data is shown in Table 19. The simulated grades in each stream can be compared directly to the measured grades shown in Table 17, and again very good correlation is observed. Stream flowrates and recoveries are comparable to the nominal flowrates and recoveries, again indicating the simulation was successful.

The data on Table 19 and Figures 15 and 16 is sufficient to validate the implementation of the simulator for the secondary grinding circuit of the Fairlane Plant

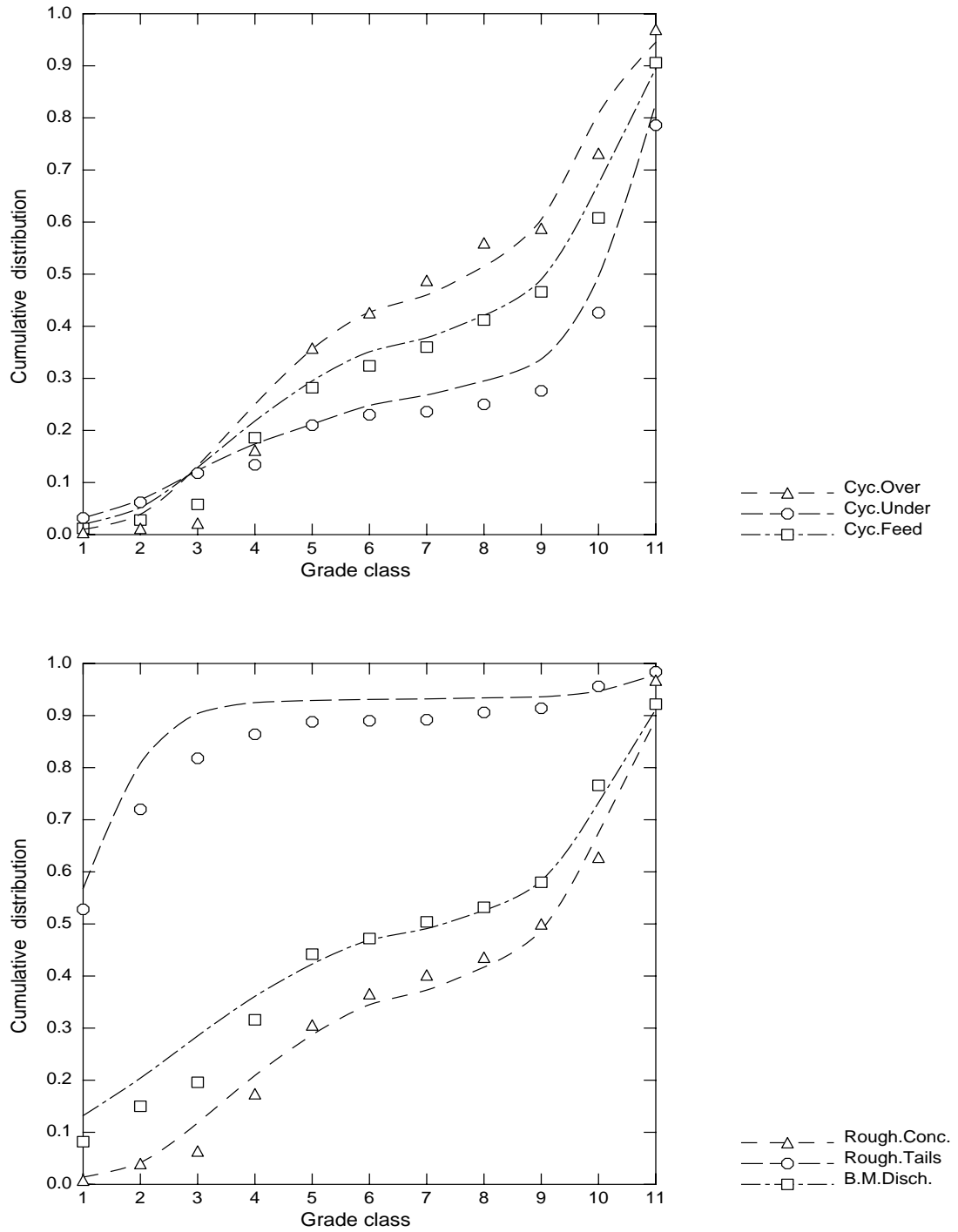


Figure 15 Comparison between measured and simulated composite grade distributions in several streams of the Fairlane Plant grinding circuit. Points show measured distributions and lines show calculated distributions

Table 19 The simulated flow rates and grades in the streams of the secondary grinding circuit of the Fairlane Plant. Recoveries are based on the total flow rates from the four feed streams

Stream	Solid Flow, Tons/hour	Water Flow, m <sup>3</sup> /hour	solids, %	Recovery of solids, %	Recovery of Chert, %	Grade of Chert, %	Recovery of Magnetite, %	Grade of Magnetite, %
Cob.Conc.	301.26	137.88	68.60	79.11	83.09	43.36	76.32	56.64
Cyc.Feed	554.04	425.16	56.58	145.50	93.24	26.76	183.04	73.24
Cyc.Under	316.66	36.83	89.58	83.16	62.08	31.19	98.09	68.67
Cyc.Over	237.89	388.44	37.98	62.47	31.16	20.84	84.94	79.16
D.D.Conc.	57.49	30.35	65.45	15.10	10.51	29.07	18.39	70.92
D.D.Tails	4.82	59.36	7.51	1.27	2.64	87.15	0.28	12.86
B.M.Disch.	675.36	205.06	76.71	177.36	166.12	39.13	185.44	60.87
Rough.Conc.	532.08	340.42	60.98	139.73	87.20	26.07	177.43	73.92
Rough.Tails	143.32	1235.52	10.39	37.64	78.93	87.62	8.01	12.39
Scav.Conc.	17.23	23.50	42.30	4.52	3.40	31.41	5.33	68.59

and the characterization of the liberation and comminution properties of the Taconite ore.

## **Discussion**

The novel procedures for liberation characterization and measurement described in this work reveal a not previously observed perspective of the interactions between the basic particle properties, namely size and composition, and the physical action of mineral processing devices. The work reported here is in fact the first successful study carried out in an industrial mineral processing plant that includes the detailed liberation characteristics of the ore.

The Taconite particles are particularly interesting to examine from this new, more detailed perspective. In Figure 17, the measured size/liberation spectrum of the Cobber Concentrate particles is shown. Approximately 47% of the particles are larger than 1000 microns, and their grade distribution was assumed to be constant and equal to the grade distribution measured in the -1000+710 micron particles. This is not a bad assumption because the larger particles tend to be in a very narrow grade range. The particles in the Cobber Concentrate stream represent the main feed stream to the grinding circuit. It is clear from the figure that the bulk of the particles, mainly in the coarser sizes, are unliberated. Below 106 microns, most particles are in the higher grade classes, but not many liberated particles of either phase are present. The transition between this quasi liberation state and no liberation occurs between 106 and 710 microns, with the spreading of the grade spectrum. The presence of very few liberated or quasi liberated chert particles is due to the action of the Cobber magnetic separator, a high intensity wet magnetic drum separator. The few liberated chert particles must result from by-pass

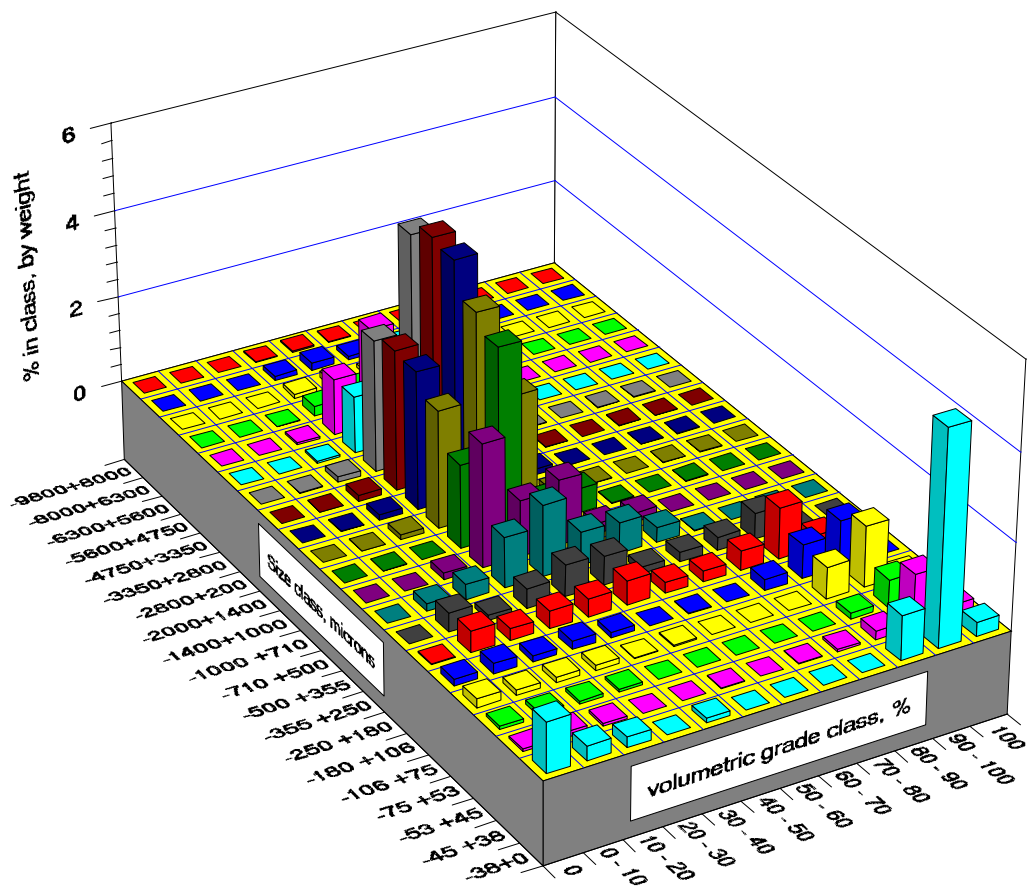


Figure 17 The particle size/grade spectrum in the Cobber Concentrate stream

phenomena in the Cobber separator. In the figure, the basic liberation characteristics of the Taconite ore can be observed, like the fast transition from unliberated to quasiliberated, and also the slow transition from quasiliberated to liberated in the magnetite end, giving rise to the liberation model modifications in Equations 1 and 2.

The measured and simulated size/grade spectrum in the Ball Mill Discharge is shown in Figure 18. In this stream the particles are comparatively finer, with approximately 97% of the particles smaller than 1000 microns, due to the comminution in the ball mill. The calculated spectrum is considerably smoother than the measured spectrum, and the main reason for this is the smooth nature of the liberation model, which is continuous in both size and grade domains, and consequently dampens the noise from stereological correction that is imputed through the measured spectrum of the feed streams. In the ball mill, a significant fraction of liberated particles of both phases is generated, and the bulk of these particles are found below 75 microns. This small "liberation size" characterizes the difficulty of processing the Taconite ore. In the ball mill discharge, the bulk of the particles are unliberated, and these must be recirculated to regrind. The ball mill discharge constitutes the feed stream to the Rougher separation, and the objective of this separation stage is to discard the lower grade and liberated Chert particles. The measured and simulated size/grade spectrum in the Rougher Tails stream is shown in Figure 19, and from this perspective it is clear that the Rougher is indeed discharging the lower grade and the liberated Chert particles in the tails stream. The concentrate stream must contain the remaining particles, and this is clearly shown in Figure 20. Very few high grade particles remain in the Rougher tails stream and very

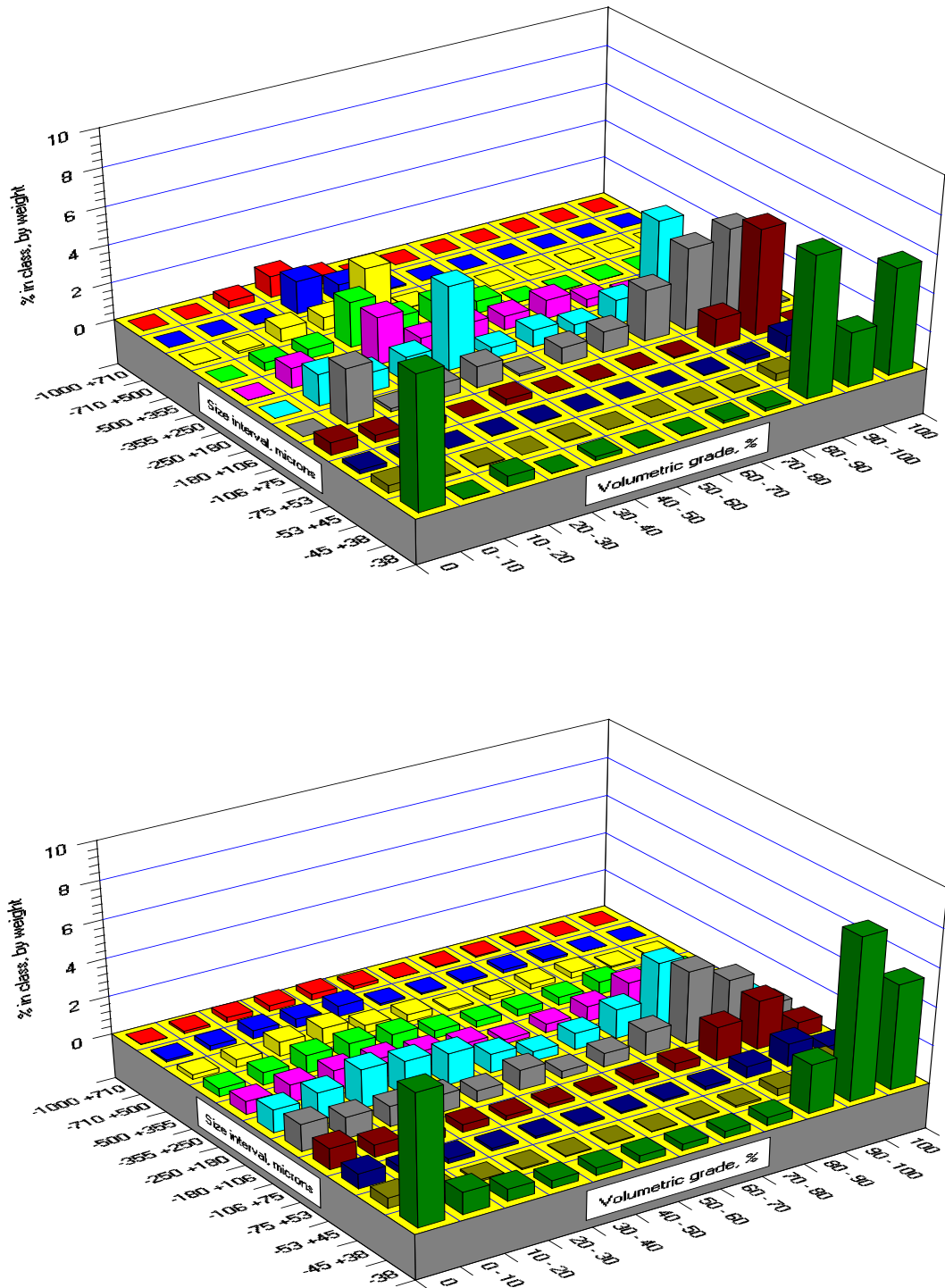


Figure 18 The measured (top) and simulated (bottom) particle size/grade spectrum in the Ball Mill Discharge

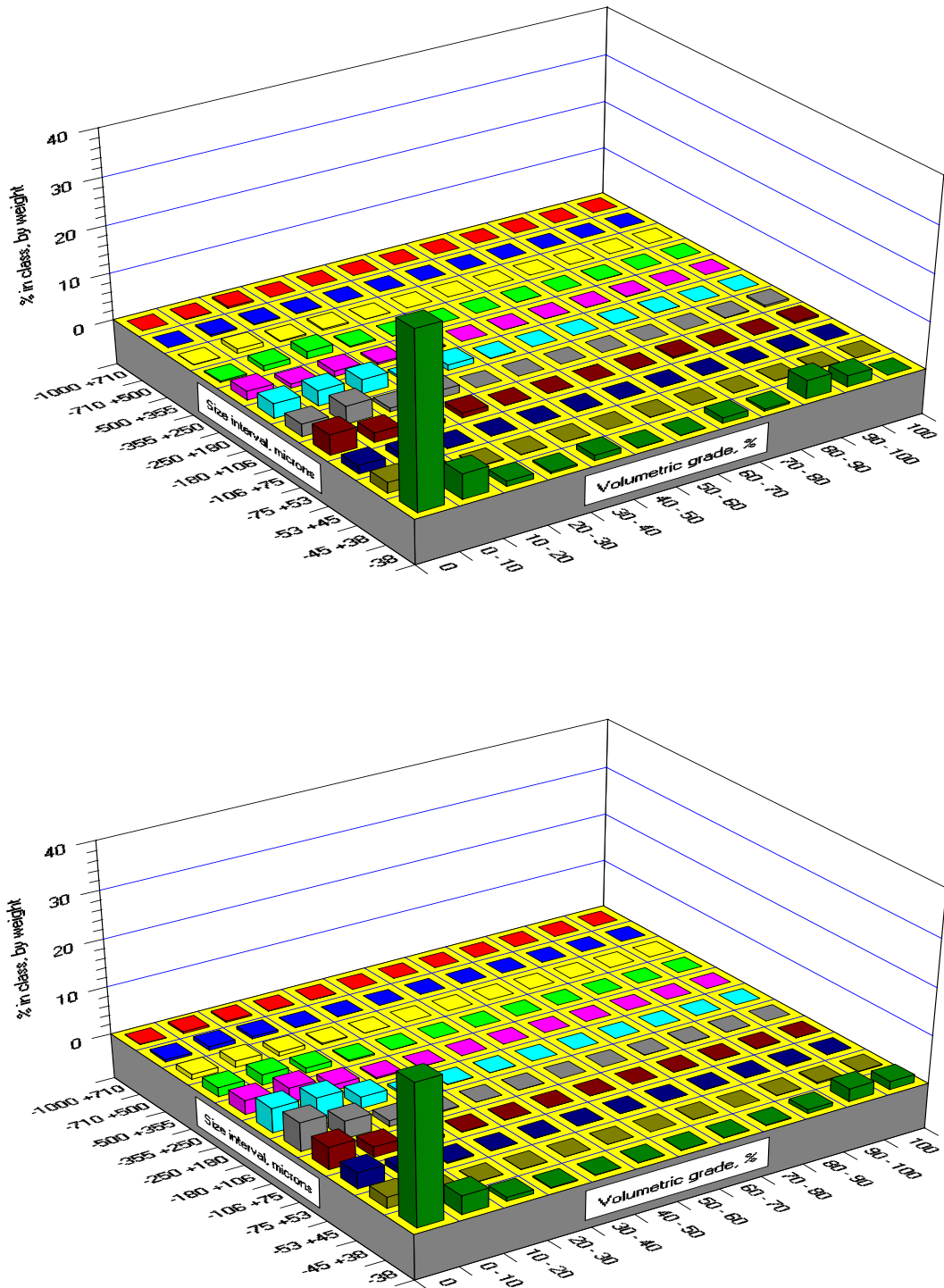


Figure 19 The measured (top) and simulated (bottom) particle size/grade spectrum in the Rougher Tails

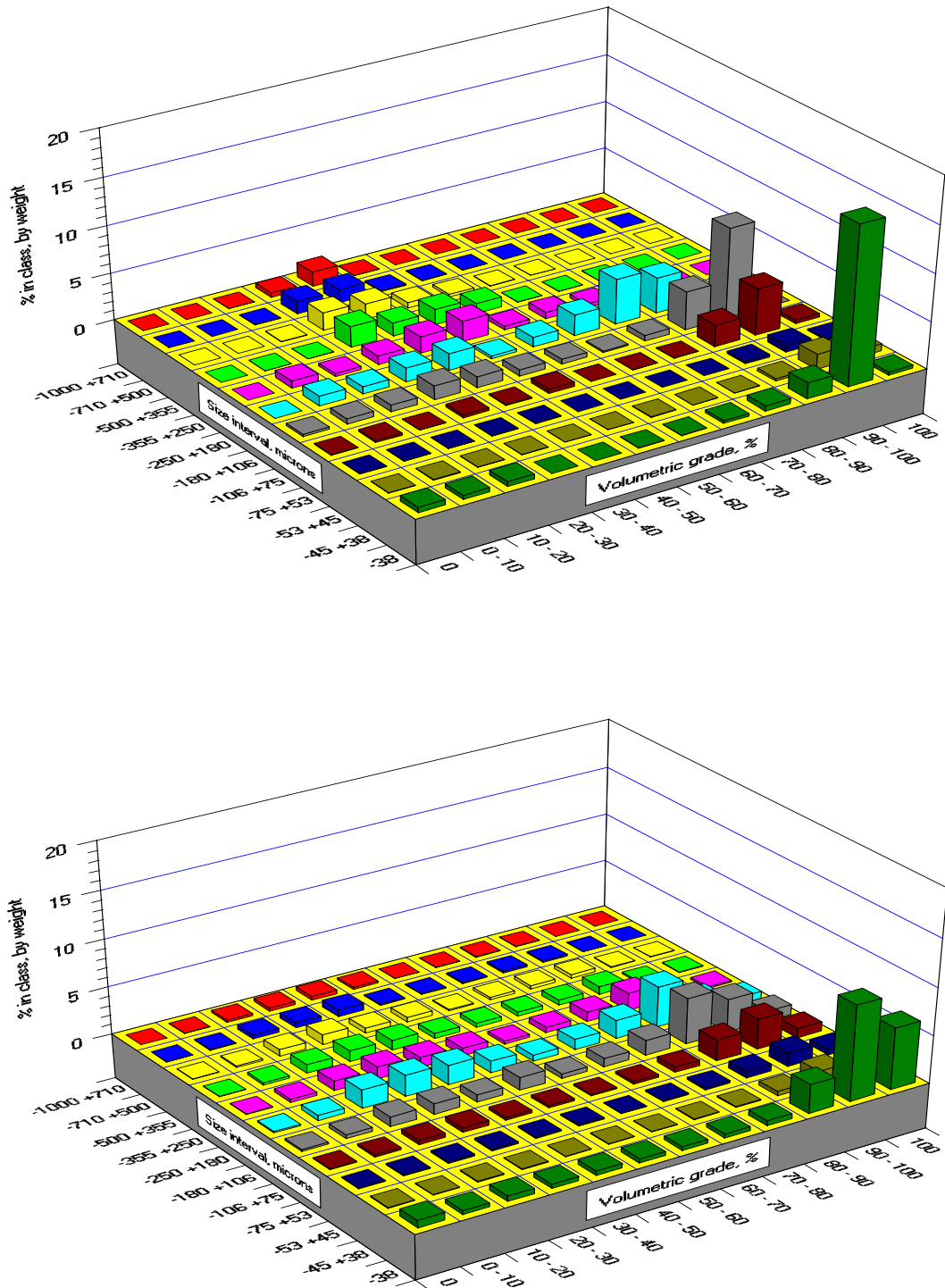


Figure 20 The measured (top) and simulated (bottom) particle size/grade spectrum in the Rougher Concentrate

few low grade particles remain in the concentrate stream, and this is mostly due to the high by-pass fraction in the separation. The bulk of the unliberated particles follow the concentrate stream, and this is beneficial, since the unliberated particles must undergo regrind before they leave the circuit. The sharp separation at low grade is characteristic of wet magnetic drum separators, which tend to direct particles that contain even a small fraction of a strong magnetic phase, in this case Magnetite, to the concentrate stream, and thus the low separation grade used in the model. Again, for both concentrate and tails streams, the measured and simulated spectra are in very good concordance. The Scavenger Concentrate and the Dewatering Drum Tails particles, shown in Figure 21, are added to the Rougher Concentrate to form the Cyclone Feed stream. The particles from these two subsidiary feed streams represent less than 5% of the Cyclone Feed. The Scavenger Concentrate particle distribution resembles that of the Rougher Concentrate particles, and this indicates that a fraction of the by-passed Magnetite containing particles in the Rougher separation are successfully returned to the grinding circuit. The Dewatering Drum Tails particles are mostly oversize particles from the double-deck vibrating screens, and some fine, screen by-pass particles. The bulk of the stream is of low grade, and liberated Chert particles. Perhaps, a better configuration for the circuit would be to restream these particles to the Rougher feed stream, so that they are discharged before they return to the Ball Mill.

Over 95% of the Cyclone Feed particles are Rougher Concentrate particles. The measured and simulated particle size/grade spectra in the Cyclone Feed stream are shown in Figure 22, and these must be comparable to the spectra in Figure 20. The Cyclone

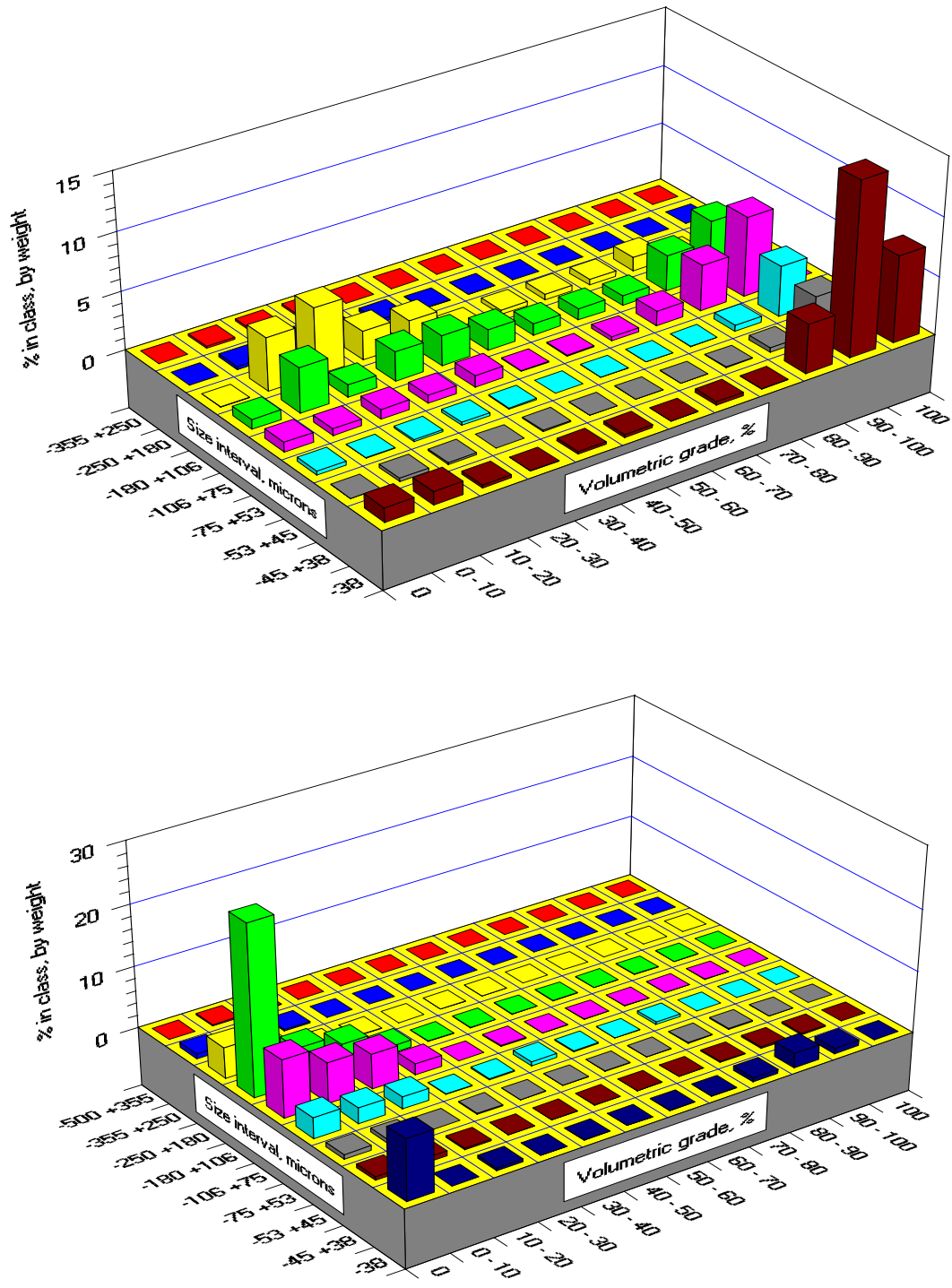


Figure 21 The measured particle size/grade spectrum in the Scavenger Concentrate (top) and Dewatering Drum Tails (bottom) streams

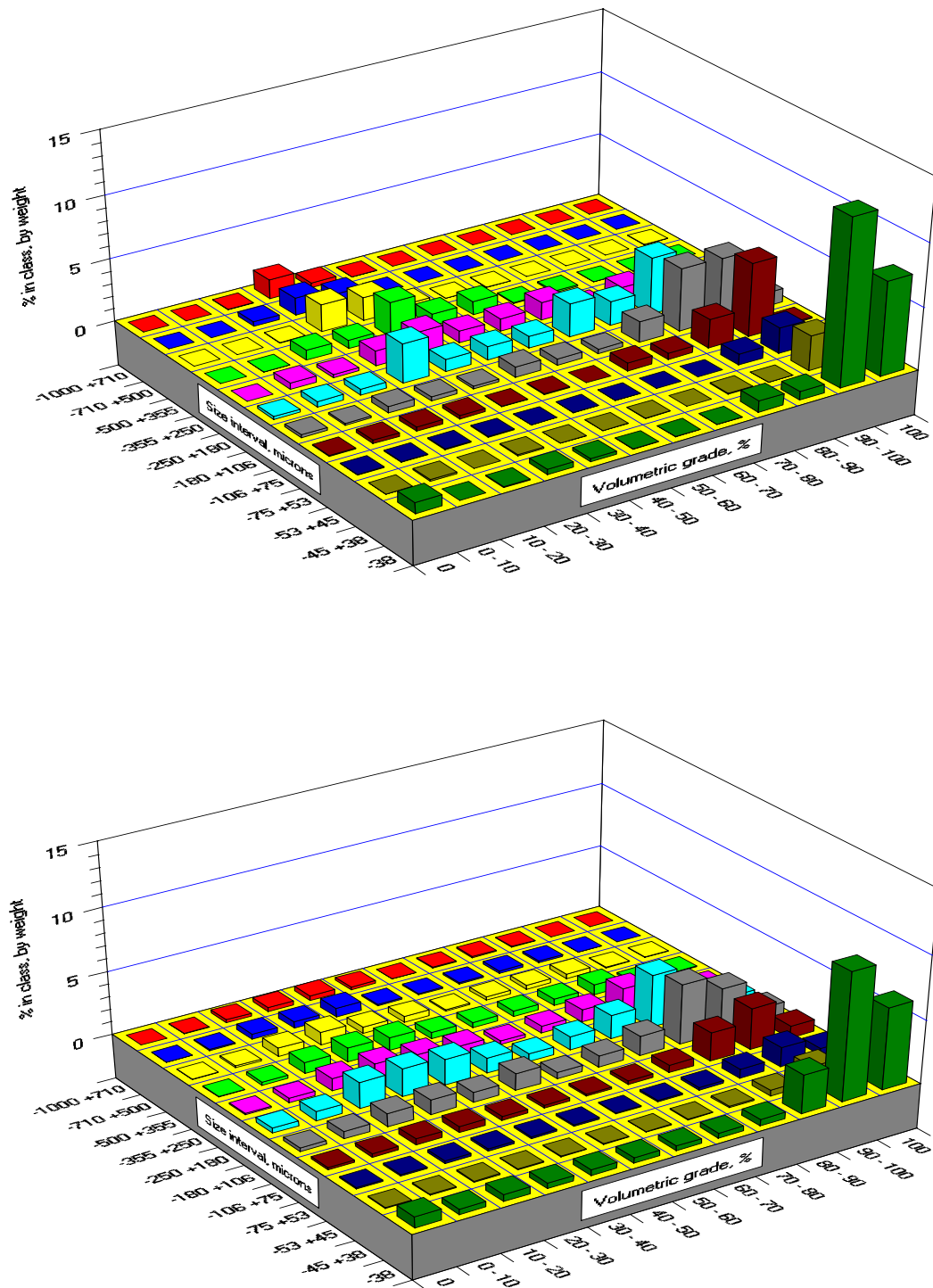


Figure 22 The measured (top) and simulated (bottom) particle size/grade spectrum in the Cyclone Feed stream

Feed is a particularly difficult stream to sample, and good, representative samples can only be obtained from the cyclone cluster feed head, with the sampling probe introduced down to a well mixed region of the incoming slurry flow. Comparison between the measured spectra in Figures 20 and 22 indicates that a good sample was obtained in the Cyclone Feed stream, and this data was used to calibrate the Hydrocyclone model. Again, there is very good agreement between the measured and simulated spectra corresponding to the Cyclone Feed stream.

The calculated and measured size/grade spectra in the Hydrocyclone Overflow stream is shown in Figure 23. These particles are the finished product of the secondary grinding circuit. The bulk of the particles is smaller than 106 microns, attending the specification for pellet making. Most particles are high grade and liberated Magnetite particles. Some contamination from larger, lower grade particles is observed, and this is probably due to short circuiting to the overflow in the Hydrocyclone. There is, once again, very good agreement between measured and simulated spectra. In contrast, the coarser, unliberated particles must be observed in the Hydrocyclone Underflow stream. This is shown in Figure 24, and the measured and calculated spectra confirm this premise. This is good, because unliberated particles must be redirected to regrind, and the underflow stream is, in fact, one of the main contributions to the ball mill feed stream. However, Figure 24 also shows clearly the expected concentration effect due to the differential density between Chert and Magnetite, and a large fraction of intermediate size, high grade and liberated Magnetite particles are also found in the Underflow. This is not desired, since it is costly and uneconomic to regrinding particles

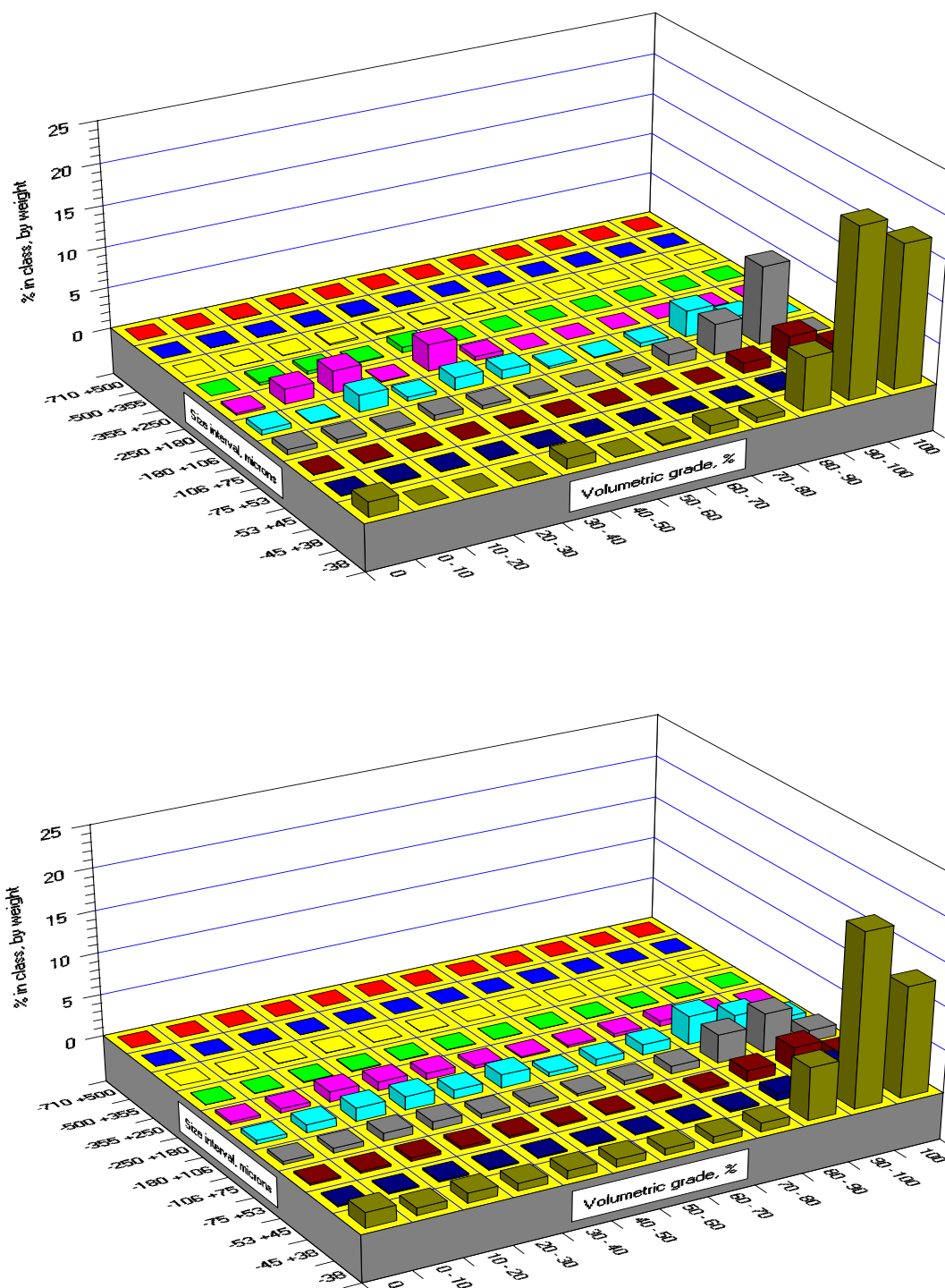


Figure 23 The measured (top) and simulated (bottom) particle size/grade spectrum in the Cyclone Overflow stream

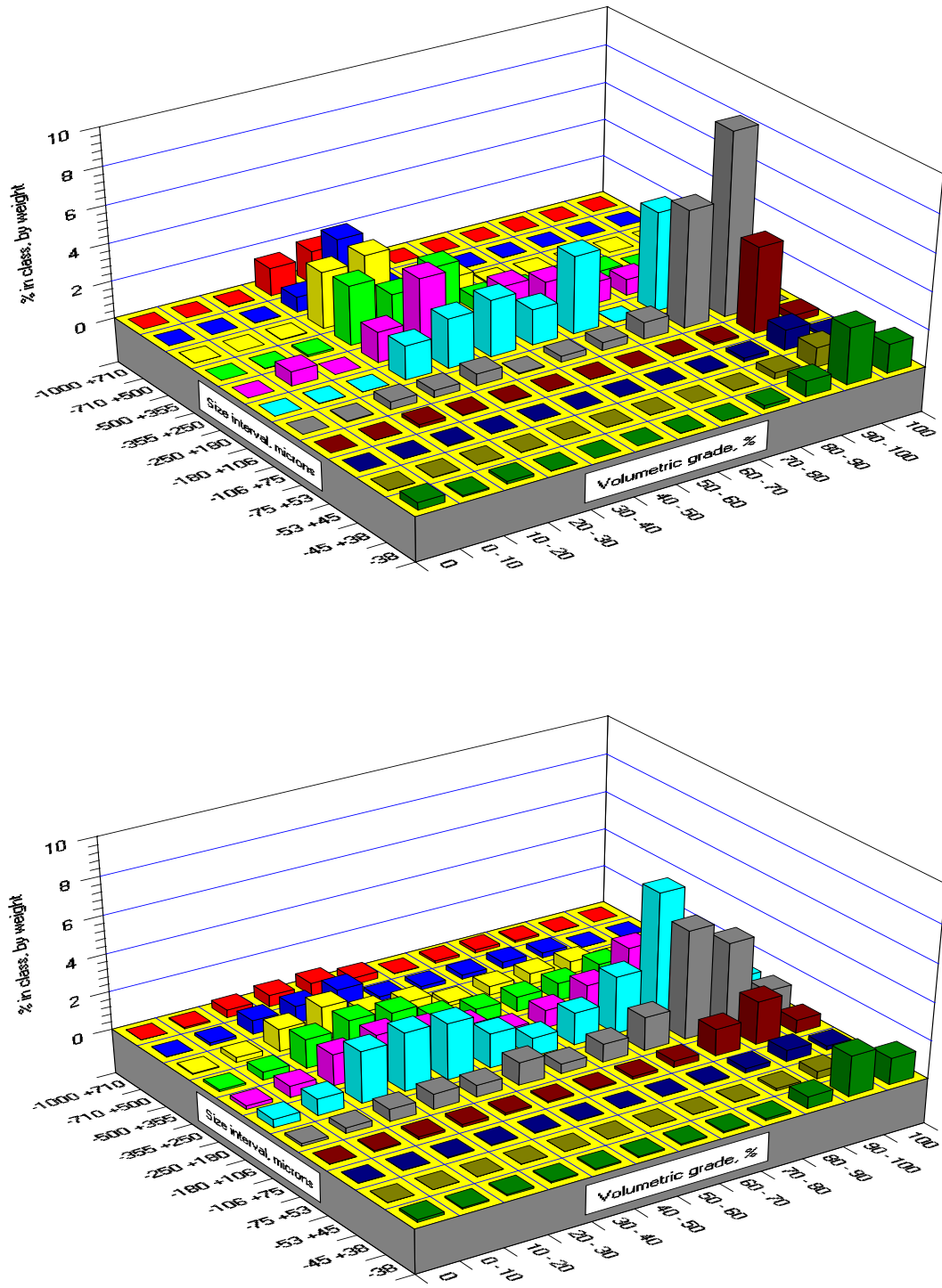


Figure 24 The measured (top) and simulated (bottom) particle size/grade spectrum in the Cyclone Underflow stream

that are already at product specification. This is probably the most important finding of this study, from the point of view of troubleshooting and plant optimization. Further work must be directed at minimizing the regrind of these particles, with great potential for economic improvement.

Finally, to complete the sweep through the streams involved in this grinding circuit with the new perspective that only this kind of detailed liberation analysis can provide, the measured size/grade spectrum in the Dewatering Drum Concentrate stream is shown in Figure 25. These particles complete, together with Cyclone Underflow and Cobber Concentrate, the feed stream to the Ball Mill. This is the final subsidiary feed stream, and the particles here represent less than 9% of the feed to the Ball Mill. However, once again, fine, high grade and liberated Magnetite is redirected to regrind through this stream. This may be subject to appreciation for plant reconfiguration.

The work reported here was, with no doubt, extremely successful, from any point of view, starting with the planing of the sampling campaign, and ending with the discussion above. Every procedure worked satisfactorily, including stereological correction with the symmetric transformation kernel, the liberation model and its implementation in MODSIM. The simulation of the unitary operations and of the entire secondary grinding circuit have been validated, and they were good.

### **Summary and Conclusions**

Modern mineral processing plant simulation techniques can be used to minimize energy consumption while maximizing recovery of iron content from Taconite ore bodies. Essential to such study is the detailed and accurate characterization of the comminution

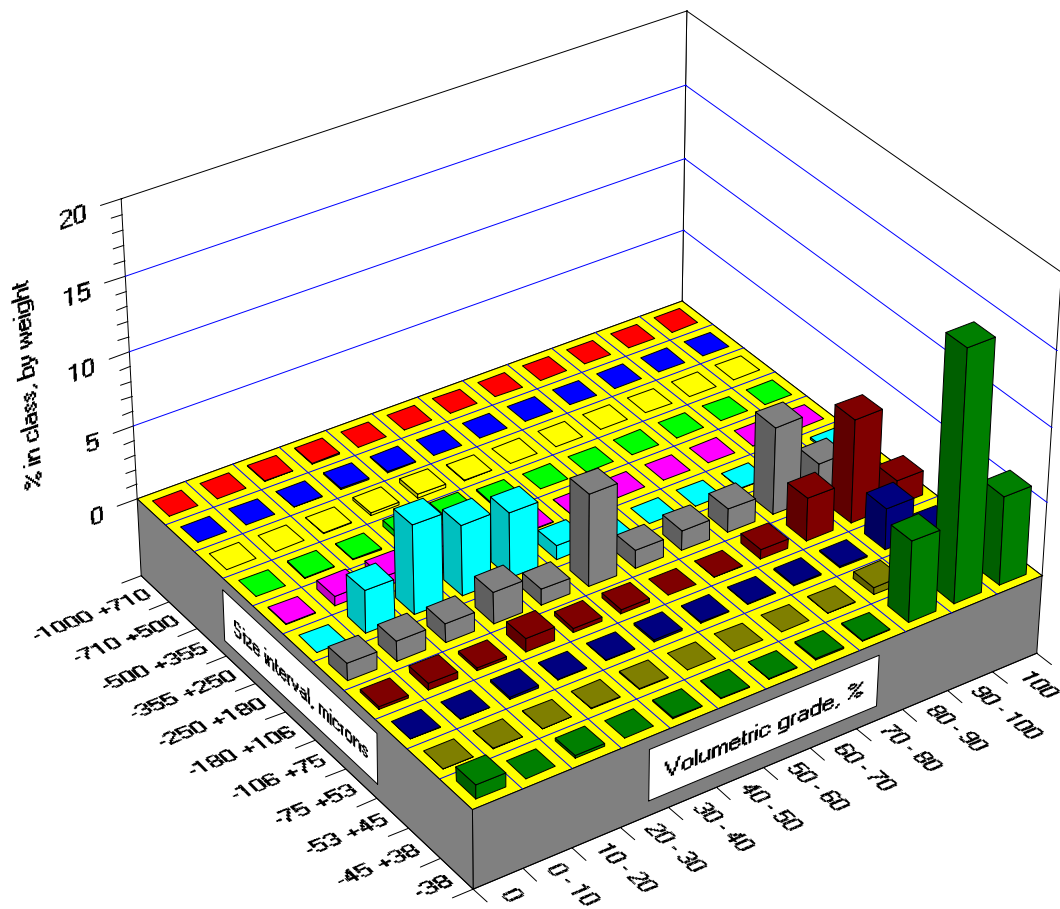


Figure 25 The measured particle size/grade spectrum in the Dewatering Drum Concentrate stream

and liberation properties of the Taconite and the accurate calibration of each of the unit operations in the grinding and concentration circuits. This report covers both the characterization of the comminution and liberation properties of the Taconite ore and the calibration of each of the unit operations in the Fairlane Plant secondary grinding circuit. The Taconite ore is very favorable for liberation studies, with respect to composition and texture. The sampling campaign at the Fairlane Plant was successful and the results in general are excellent.

The following conclusions can be drawn from this campaign.

1. The work reported here demonstrates that it is possible to model accurately the liberation of the minerals in the Fairlane Plant secondary grinding circuit.
2. A few empirical parameters are required to model the unit operations in the circuit. These parameters can be determined from the measured size/grade spectra in the circuit streams, with the selection of appropriate models and an optimization procedure.
3. The mineralogical texture of the Taconite ore was characterized completely by direct observation using image analysis. These results are not restricted, and can be used for any ore body in the Mesabi Iron Range of similar formation.
4. This study demonstrated that it is possible to measure the liberation spectra accurately in many size fractions in several plant streams using standard image analysis techniques with stereological correction. These spectra were used to confirm the validity of the simulation and provided immediate indications of where improvements in the overall plant performance might be sought.

5. The simulator can form the basis for the determination of an overall economic optimum for the process as a whole.

### **Future Work**

Potential for reduction of mill power draft in the plant has been determined. The detailed characterization reported here has indicated two separate sources of potential improvement. The first issue to be addressed is the reconfiguration of the Dewatering Drum streams, which may represent a reduction of up to 10% of mill power draft. The second issue is with respect to the recirculation of liberated magnetite in the hydrocyclone underflow. It is possible, by setting appropriate operational conditions, that the amount of recirculating liberated and nearly liberated magnetite be reduced by a significant fraction, with proportional reduction of the power draft of the mill. The simulator will be used to assess these issues.

**APPENDIX**

**MEASURED LINEAR GRADE DISTRIBUTIONS IN THE  
TACONITE ORE SAMPLES FROM THE FAIRLANE  
PLANT SECONDARY GRINDING CIRCUIT  
STREAMS**

Table 1 The measured, conditional on size, linear grade distributions by length in the Ball Mill Discharge stream sample

Particle size range, microns											
linear grade, %	-1000 +710	-710 +500	-500 +355	-355 +250	-250 +180	-180 +106	-106 +75	-75 +53	-53 +45	-45 +38	-38
0	31.76	30.78	34.63	38.28	40.30	32.44	28.07	24.39	35.74	27.70	46.66
0-10	14.15	11.01	10.44	7.89	5.19	4.63	3.12	1.75	2.41	1.33	0.48
10-20	13.69	12.24	9.67	7.76	6.39	4.88	2.97	1.23	1.30	0.98	0.47
20-30	9.05	9.92	9.09	7.24	5.71	4.67	2.53	1.26	0.86	0.90	0.39
30-40	7.29	8.11	7.48	5.76	4.88	4.68	2.05	1.17	0.95	0.81	0.51
40-50	4.76	5.73	5.24	5.16	4.69	4.06	2.64	0.96	0.87	1.29	0.40
50-60	4.48	4.98	5.15	4.68	5.01	4.14	3.24	1.52	1.36	1.28	0.63
60-70	3.23	4.13	3.46	4.00	4.21	4.25	3.31	1.44	1.51	1.33	1.20
70-80	2.89	3.14	3.05	3.69	3.93	4.22	3.63	2.47	2.05	1.74	1.69
80-90	2.26	2.41	3.05	3.48	4.25	5.67	6.17	4.22	3.27	2.75	3.45
90-100	1.52	1.70	2.25	2.69	3.40	5.81	8.21	7.75	6.23	6.03	6.83
100	4.92	5.85	6.49	9.37	12.04	20.55	34.06	51.84	43.45	53.86	37.29

Table 2 The measured, conditional on size, linear grade distributions by length in the Cobber Concentrate stream sample

Particle size range, microns											
linear grade, %	-1000 +710	-710 +500	-500 +355	-355 +250	-250 +180	-180 +106	-106 +75	-75 +53	-53 +45	-45 +38	-38
0	25.13	26.59	30.99	32.80	33.64	31.42	29.26	26.25	30.44	18.04	32.08
0-10	10.49	9.71	9.04	7.15	5.86	4.48	2.51	1.62	2.70	1.64	1.28
10-20	11.08	10.43	9.22	7.66	5.10	4.43	2.24	1.96	1.56	0.68	0.66
20-30	9.44	9.05	7.64	6.78	5.49	4.01	2.27	1.25	1.30	0.74	0.78
30-40	6.86	6.80	6.37	6.74	4.56	3.67	1.79	1.32	0.98	0.67	0.48
40-50	5.74	6.22	5.39	5.50	4.54	3.57	1.89	0.89	1.20	1.07	0.51
50-60	4.81	5.63	5.28	5.41	4.94	3.90	2.30	1.47	1.10	1.42	1.07
60-70	4.93	4.18	5.29	4.47	4.23	3.91	2.46	1.70	1.39	1.60	1.25
70-80	4.16	4.09	4.40	4.12	4.25	4.03	3.29	2.92	1.98	1.91	2.23
80-90	4.00	4.50	3.75	4.11	4.96	4.71	4.56	4.96	3.32	3.45	4.80
90-100	3.50	3.35	2.98	2.74	4.20	4.48	6.52	9.23	7.50	8.84	10.14
100	9.86	9.45	9.65	12.52	18.23	27.39	40.91	46.43	46.53	59.94	44.72

Table 3 The measured, conditional on size, linear grade distributions by length in the Cyclone Feed stream sample

Particle size range, microns											
linear grade, %	-1000 +710	-710 +500	-500 +355	-355 +250	-250 +180	-180 +106	-106 +75	-75 +53	-53 +45	-45 +38	-38
0	29.97	32.11	30.98	31.74	28.91	25.10	13.57	12.60	10.60	8.93	9.77
0-10	13.36	11.96	9.80	6.38	5.71	3.81	1.51	1.52	0.99	0.97	0.62
10-20	12.86	13.38	10.75	7.80	6.19	3.98	2.06	1.56	1.03	0.81	0.35
20-30	11.13	9.84	8.44	7.81	5.96	4.41	2.50	1.39	1.18	0.64	0.72
30-40	7.03	7.48	7.03	6.25	5.59	4.62	2.36	1.68	1.07	0.77	0.66
40-50	5.23	4.62	5.13	5.85	4.73	3.67	2.24	1.97	1.40	0.61	0.57
50-60	4.75	4.17	5.06	5.32	4.65	4.78	2.70	2.32	1.57	1.00	1.02
60-70	3.64	3.65	4.31	4.48	4.82	4.83	3.23	2.74	2.11	1.63	1.70
70-80	2.90	2.78	3.72	4.38	5.34	4.68	3.76	2.80	2.48	2.17	2.64
80-90	2.17	2.01	3.11	4.48	4.43	5.16	4.67	4.84	5.33	4.18	4.78
90-100	1.46	1.41	2.48	3.21	4.64	5.11	7.33	7.50	8.52	7.83	9.01
100	5.50	6.59	9.19	12.30	19.03	29.85	54.07	59.08	63.72	70.46	68.16

Table 4 The measured, conditional on size, linear grade distributions by length in the Cyclone Overflow stream sample

Particle size range, microns										
linear grade, %	-710 +500	-500 +355	-355 +250	-250 +180	-180 +106	-106 +75	-75 +53	-53 +45	-45 +38	-38
0	38.47	33.43	35.03	51.61	55.48	34.33	17.13	8.86	9.19	9.43
0-10	11.44	8.03	6.47	6.50	6.36	4.18	1.53	0.88	0.88	0.39
10-20	13.19	9.31	8.27	7.30	6.39	4.14	1.38	0.67	0.78	0.47
20-30	10.18	8.83	7.04	6.49	5.45	4.64	1.82	0.81	0.96	0.80
30-40	6.37	7.80	6.28	5.11	4.88	3.89	1.64	0.99	0.92	0.81
40-50	5.26	6.99	6.55	3.78	3.58	3.28	1.76	0.97	0.50	0.70
50-60	4.39	5.59	5.71	3.55	2.70	2.87	1.93	1.29	0.72	1.21
60-70	2.72	4.99	5.15	2.33	2.23	3.34	2.77	1.78	1.23	1.92
70-80	2.08	4.11	4.53	2.40	2.09	3.63	2.79	2.62	1.57	1.80
80-90	1.30	3.25	3.12	2.53	2.04	4.08	4.46	3.93	3.63	4.17
90-100	0.61	1.80	2.52	1.69	1.40	5.52	6.70	7.97	6.23	8.76
100	3.99	5.87	9.33	6.71	7.40	26.10	56.09	69.23	73.39	69.54

Table 5 The measured, conditional on size, linear grade distributions by length in the Cyclone Underflow stream sample

Particle size range, microns											
linear grade, %	-1000 +710	-710 +500	-500 +355	-355 +250	-250 +180	-180 +106	-106 +75	-75 +53	-53 +45	-45 +38	-38
0	26.47	26.96	30.08	28.32	27.84	16.67	8.36	5.63	6.96	6.86	16.77
0-10	11.63	9.14	9.01	6.11	4.72	3.25	1.36	1.18	1.16	0.84	0.62
10-20	13.39	10.87	9.31	7.72	6.44	4.46	1.51	1.10	0.77	0.63	0.47
20-30	9.47	9.91	7.96	7.63	5.54	3.95	1.66	0.66	0.95	0.49	0.54
30-40	7.36	7.01	6.90	6.49	6.16	4.70	2.00	0.89	1.07	0.58	0.55
40-50	6.14	5.95	5.71	5.42	5.16	4.72	1.76	1.10	1.16	0.97	0.80
50-60	4.55	5.64	5.79	5.43	5.61	4.41	2.60	1.03	1.84	1.15	1.12
60-70	3.14	5.29	4.58	5.02	5.38	4.53	2.83	1.52	1.72	1.66	1.51
70-80	3.21	3.88	4.21	4.73	4.47	4.94	3.89	2.21	2.32	1.99	2.23
80-90	3.38	3.33	3.48	4.69	5.62	5.67	6.46	4.94	4.18	4.32	4.17
90-100	2.57	2.61	3.13	3.77	4.13	5.34	9.14	9.67	9.40	9.90	10.01
100	8.69	9.41	9.84	14.67	18.93	37.36	58.43	70.07	68.47	70.61	61.21

Table 6 The measured, conditional on size, linear grade distributions by length in the Dewatering Drum Concentrate stream sample

Particle size range, microns											
linear grade, %	-1000 +710	-710 +500	-500 +355	-355 +250	-250 +180	-180 +106	-106 +75	-75 +53	-53 +45	-45 +38	-38
0	33.72	32.40	31.89	39.11	56.14	51.92	30.93	14.89	10.14	4.97	8.49
0-10	15.81	11.53	9.08	6.52	6.39	7.20	3.63	1.61	1.45	0.60	0.32
10-20	15.29	11.79	9.77	8.56	7.11	8.00	4.28	1.80	1.49	0.93	0.36
20-30	9.88	8.96	8.50	7.44	6.23	6.37	3.84	2.04	1.47	0.67	0.48
30-40	7.15	7.11	7.59	6.90	4.65	4.60	4.33	1.40	1.50	1.03	0.82
40-50	4.97	6.52	6.88	5.57	3.45	3.53	3.91	1.82	1.74	0.85	0.73
50-60	3.95	5.25	6.12	5.26	2.91	3.13	4.55	1.93	1.96	1.07	1.35
60-70	2.84	4.29	4.81	5.01	2.54	2.52	4.03	1.98	1.73	1.51	1.51
70-80	2.20	3.16	3.37	3.52	2.02	1.80	3.68	2.45	2.52	2.00	2.34
80-90	1.52	2.52	2.90	3.04	1.92	1.62	4.85	4.11	3.36	4.14	4.70
90-100	0.36	1.38	1.87	2.08	0.89	1.42	5.11	5.93	6.18	6.59	11.00
100	2.31	5.09	7.22	6.99	5.75	7.89	26.86	60.04	66.46	75.64	67.90

Table 7 The measured, conditional on size, linear grade distributions by length in the Dewatering Drum Tails stream sample

Particle size range, microns									
linear grade, %	-500 +355	-355 +250	-250 +180	-180 +106	-106 +75	-75 +53	-53 +45	-45 +38	-38
0	71.38	83.03	88.49	86.62	82.18	77.98	75.49	70.37	81.38
0-10	12.01	6.09	4.96	5.07	4.03	3.48	3.12	3.90	0.37
10-20	5.67	4.43	2.98	3.39	2.93	3.01	2.22	2.42	0.49
20-30	3.00	2.59	1.42	1.73	2.18	1.93	1.79	1.63	0.52
30-40	2.23	1.33	0.73	1.20	1.52	1.61	1.43	1.02	0.42
40-50	1.48	0.56	0.37	0.51	1.62	1.59	1.24	0.80	0.45
50-60	1.11	0.72	0.36	0.36	1.31	1.58	1.34	1.08	0.52
60-70	0.81	0.37	0.23	0.27	0.90	1.66	1.39	1.07	1.08
70-80	0.39	0.15	0.15	0.14	0.44	1.17	1.17	1.61	1.09
80-90	0.59	0.19	0.06	0.15	0.51	1.26	1.57	2.42	1.55
90-100	0.50	0.13	0.08	0.16	0.56	0.91	1.19	2.29	1.09
100	0.83	0.41	0.17	0.40	1.82	3.82	8.05	11.39	11.04

Table 8 The measured, conditional on size, linear grade distributions by length in the Rougher Concentrate stream sample

Particle size range, microns											
linear grade, %	-1000 +710	-710 +500	-500 +355	-355 +250	-250 +180	-180 +106	-106 +75	-75 +53	-53 +45	-45 +38	-38
0	24.29	29.34	29.97	29.33	33.16	24.62	18.58	11.19	12.73	10.59	12.08
0-10	11.57	10.37	9.48	6.92	5.07	3.97	2.76	1.29	1.17	1.12	0.94
10-20	13.26	10.43	9.44	8.53	6.35	4.20	2.70	1.68	1.28	0.67	0.70
20-30	9.74	8.82	8.10	7.85	6.13	4.08	3.02	1.51	1.31	0.74	0.60
30-40	8.15	6.79	6.59	6.75	5.47	3.80	2.27	1.78	1.44	1.03	0.51
40-50	5.91	5.97	5.55	6.76	5.48	3.79	2.31	1.47	0.96	0.94	0.66
50-60	5.72	5.41	5.86	5.11	4.81	4.42	2.58	1.26	1.42	1.80	1.21
60-70	4.42	4.54	4.59	4.56	4.32	5.41	2.63	2.27	1.60	1.31	2.28
70-80	3.20	3.84	4.07	3.85	4.13	5.03	2.97	2.83	2.26	1.74	2.75
80-90	3.10	3.23	3.96	4.45	4.05	5.87	4.09	4.81	3.69	3.37	6.28
90-100	2.55	2.85	2.95	3.18	3.67	5.11	6.03	8.08	7.98	8.09	10.81
100	8.09	8.41	9.44	12.71	17.36	29.70	50.06	61.83	64.16	68.60	61.18

Table 9 The measured, conditional on size, linear grade distributions by length in the Rougher Tails stream sample

Particle size range, microns											
linear grade, %	-1000 +710	-710 +500	-500 +355	-355 +250	-250 +180	-180 +106	-106 +75	-75 +53	-53 +45	-45 +38	-38
0	54.92	59.54	63.92	64.62	78.48	76.17	77.79	81.63	85.42	88.41	87.21
0-10	15.61	14.92	11.67	10.20	5.97	5.25	4.54	3.07	2.80	1.48	1.13
10-20	9.73	8.78	8.05	7.27	3.90	4.32	3.07	2.21	1.23	0.88	0.86
20-30	5.99	5.27	4.82	4.53	2.78	2.53	2.59	1.75	1.05	0.57	0.40
30-40	3.39	3.82	3.42	2.65	1.56	1.51	1.20	1.20	0.74	0.59	0.59
40-50	2.53	2.07	2.13	2.09	1.28	1.65	1.08	1.05	0.66	0.57	0.33
50-60	1.42	1.27	1.53	1.54	1.19	1.59	0.83	0.84	0.80	0.72	0.66
60-70	1.03	1.13	1.04	1.37	0.76	1.28	0.81	0.72	0.65	0.47	0.72
70-80	1.18	0.78	0.71	1.05	0.64	0.97	0.99	0.59	0.64	0.60	0.37
80-90	0.92	0.66	0.42	1.01	0.89	0.94	0.78	0.74	0.57	0.58	0.89
90-100	0.80	0.35	0.52	0.70	0.72	0.67	0.74	0.83	0.60	0.44	0.71
100	2.48	1.41	1.77	2.97	1.83	3.12	5.58	5.37	4.84	4.69	6.13

Table 10 The measured, conditional on size, linear grade distributions by length in the Scavenger Concentrate stream sample

Particle size range, microns								
linear grade, %	-355 +250	-250 +180	-180 +106	-106 +75	-75 +53	-53 +45	-45 +38	-38
0	57.61	55.09	55.27	39.80	23.62	18.38	15.29	15.40
0-10	10.55	7.80	8.50	4.00	2.80	1.53	1.45	1.16
10-20	7.82	7.86	6.33	4.04	2.27	1.50	1.21	0.53
20-30	6.05	5.39	4.45	4.00	2.06	1.34	1.03	0.43
30-40	3.56	4.16	3.39	3.14	2.38	1.02	0.98	0.74
40-50	2.59	3.13	2.16	3.16	1.82	1.22	1.06	0.73
50-60	2.48	2.62	2.45	2.87	2.50	1.58	1.15	1.00
60-70	1.97	2.28	2.15	3.05	2.82	1.42	1.47	1.28
70-80	1.20	1.82	2.17	2.85	2.92	2.20	2.60	2.35
80-90	1.24	1.93	2.47	3.29	5.02	3.49	3.98	4.07
90-100	0.88	1.48	1.92	3.75	6.69	6.18	6.57	10.34
100	4.05	6.44	8.74	26.05	45.10	60.14	63.21	61.97

## REFERENCES

1. Kenwalt Systems (Pty) Ltd, *SysCAD/MB Mass Balance Smoothing Package - User's Manual* (Kenwalt (Pty) Ltd., Rivonia, South Africa, 1993).
2. C.L. Schneider, *Measurement and Calculation of Liberation in Continuous Milling Circuits*, Ph.D. dissertation, Department of Metallurgical Engineering, University of Utah (1995), Chapter 2, Stereological Correction of Linear Grade Distributions for Mineral Liberation, pp. 9 - 82.
3. C.L. Schneider, *Measurement and Calculation of Liberation in Continuous Milling Circuits*, Ph.D. dissertation, Department of Metallurgical Engineering, University of Utah (1995), Chapter 4, Calculation of the Liberation Spectra Produced in a Continuous Grinding Experiment, pp. 178 - 253.
4. C.L. Schneider, *Measurement and Calculation of Liberation in Continuous Milling Circuits*, Ph.D. dissertation, Department of Metallurgical Engineering, University of Utah (1995), Chapter 3, Characterization of the Internal Structure of the Quadrivariate Breakage Function, pp. 83 - 177.
5. L.G. Austin, R.R. Klimpel and P.T. Luckie, *Process Engineering of Size Reduction: Ball Milling* (New York: AIME, 1984).
6. K.T. Hsieh and K.Rajamani, "Phenomenological Model of the Hydrocyclone: Model development and Verification," *Int. J. Miner. Process.*, (1988), 22, p. 223.
7. A.B. Cortes, *Spectral Difference: A New Method for Solving the Navier-Stokes Equations*, Ph.D. dissertation, Department of Metallurgical Engineering, University of Utah (1994).
8. A.J. Lynch and T. Rao, "Modelling and Scale-Up of Hydrocyclone Classifiers," *Proc. 11th Int. Mineral Processing Congress*, Cagliari, (1975), p. 245.
9. L. Plitt, "A Mathematical Model for the Hydrocyclone Classifier in Classification," *CIM Bulletin*, (1976), 69, p. 114.
10. R.P. King, *Modeling and Simulation of Mineral Processing Systems*, (1994), Lecture notes.